Classroom Photocopying Permission

Laboratory Safety

DISCLAIMER

Safety information is included in each chapter of the Companion as a precaution to the readers. Although the materials, safety information, and procedures contained in this book are believed to be reliable, they should serve only as a starting point for laboratory practices. They do not purport to specify minimal legal standards or to represent the policy of the American Chemical Society. No warranty, guarantee, or representation is made by the American Chemical Society, the authors, or the editors as to the accuracy or specificity of the information contained herein, and the American Chemical Society, the authors, and the editors assume no responsibility in connection therewith. The added safety information is intended to provide basic guidelines for safe practices. Therefore, it cannot be assumed that necessary warnings or additional information and measures may not be required. Users of this book and the procedures contained herein should consult the primary literature and other sources of safe laboratory practices for more exhaustive information. See page xxv in the Text 0 Preface file in the Companion Text folder for more information.

Chapter 5

Common Crystalline Structures

The X-ray diffraction experiment has been used to establish the structures of many different crystalline solids. In this chapter we describe some common crystalline extended structures, encompassing, in turn, materials that contain metallic, ionic, and covalent bonding. Also highlighted are the geometries found in extended solids, some of which are also present in discrete molecular species.

Because of the three-dimensional nature of these structures, the use of the ICE Solid-State Model Kit (SSMK, *see* Appendix 5.1), or a kit with comparable capabilities[1], is strongly recommended. *Structures whose assembly directions are included in the SSMK are indicated in this chapter by* ♦.

In presenting this material to a large classroom audience, a closed-circuit television or a video camera could be used. Styrofoam spheres[2] up to 1 foot in diameter permit construction of large models suitable for use in a large lecture hall. Data files containing the coordinates for the structures in the SSMK are available for the MacMolecule program (*see* Appendix 5.2).

Metals

Metals have played a central role in technology since before recorded history. For most of this time, the mechanical properties of metals have been the underlying reason for their usefulness. For example, gold, which

[1]Ordering information for other model kits and a computer program suitable for displaying solid-state structures is given in Supplier Information.

[2] Sold by Molecular Models (Supplier Information gives complete details).

2725-X/93/0097$14.55/1

Chapter 5

Common Crystalline Structures

The X-ray diffraction experiment has been used to establish the structures of many different crystalline solids. In this chapter we describe some common crystalline extended structures, encompassing, in turn, materials that contain metallic, ionic, and covalent bonding. Also highlighted are the geometries found in extended solids, some of which are also present in discrete molecular species.

Because of the three-dimensional nature of these structures, the use of the ICE Solid-State Model Kit (SSMK, *see* Appendix 5.1), or a kit with comparable capabilities[1], is strongly recommended. *Structures whose assembly directions are included in the SSMK are indicated in this chapter by* ♦.

In presenting this material to a large classroom audience, a closed-circuit television or a video camera could be used. Styrofoam spheres[2] up to 1 foot in diameter permit construction of large models suitable for use in a large lecture hall. Data files containing the coordinates for the structures in the SSMK are available for the MacMolecule program (*see* Appendix 5.2).

Metals

Metals have played a central role in technology since before recorded history. For most of this time, the mechanical properties of metals have been the underlying reason for their usefulness. For example, gold, which

[1]Ordering information for other model kits and a computer program suitable for displaying solid-state structures is given in Supplier Information.

[2] Sold by Molecular Models (Supplier Information gives complete details).

is most notable for its beautiful luster and resistance to corrosion, would nevertheless be of little value were it not for the fact that this metal can be easily worked into thin sheets and intricate shapes. The modern widespread use of metals as electrical conductors would not be practical if metals could not be drawn into wires. The ductility of metals (their ability to be formed into new shapes) derives from the nondirectionality of the metallic bond. In this section we explore the basic structures of metals that result in their remarkable mechanical properties. Microstructural defects in metals, which provide the mechanistic basis for these properties, are discussed in Chapter 6.

Metal atoms can be regarded as hard spheres for purposes of modeling them as they pack together to form a solid (recognizing that their size is actually "fuzzy," as noted in the STM description of Chapter 2). Most of the elemental metal crystal structures can be modeled by simple sphere-packing arrangements♦.

Metallic bonding is, for the most part, nondirectional. For many metals, therefore, the metal atoms arrange themselves to achieve the most efficient packing and the densest structure. Such metals will either be face-centered cubic (e.g., Al, Cu, and Au) or hexagonal close-packed (e.g., Mg, Zn, and Ti). Covalent bonds, such as those in diamond, lead to a relatively open structure dictated by the angles of the bonds. Thus, the types of bonding in materials are reflected in crystal structure.

Two-Dimensional Packing

The most efficient way to arrange spheres (circles in two dimensions) in a plane is hexagonal packing. In this arrangement, six outer circles can be arranged so that they touch a central circle. The outer circles touch so as to form a regular hexagon about the central one. Alternatively, less efficient square packing may be used to arrange the circles. Close-packing and square-packing arrays are shown in Figure 5.1 with a unit cell superimposed on each.

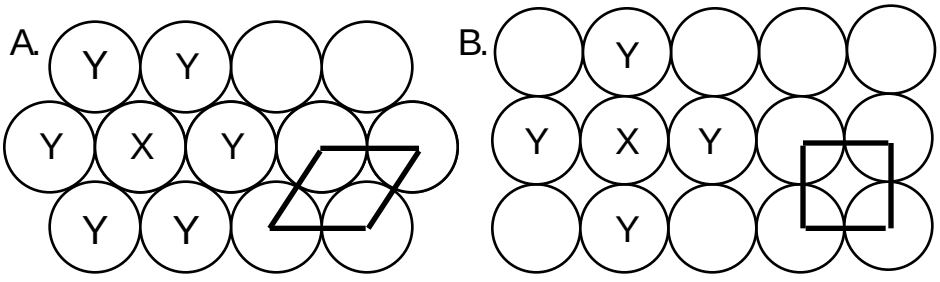

Figure 5.1. Packing arrangements in two dimensions. For an arbitrary atom marked with an X, the nearest neighbors are indicated with a Y. A unit cell is superimposed on each array. A: Close packing. B: Square packing.

The unit cell can be used to determine the "packing efficiency" of each structure. Packing efficiency in two dimensions can be related to the density of atoms (units of atoms per square centimeter):

$$\frac{\text{area of circles in the unit cell}}{\text{area of unit cell}} \times 100\% = \%\ \text{packing efficiency} \qquad (1)$$

Close packing produces, as the name implies, a denser structure. The unit cell shown for the close-packed hexagonal array (Figure 5.1A) comprises a total of one circle (Chapter 3 presents a discussion of unit-cell occupancy in structures in which the angles are not 90°) and has a packing efficiency of ~91%. For square packing, the packing efficiency is about 79%.

Another important characteristic of packing is the coordination number, or number of nearest-neighbor circles to any of the packed circles. In the close-packed structure, the coordination number is six; any arbitrarily chosen circle within the close-packed structure (one has been marked with an X) is surrounded by six nearest neighbors (marked with a Y). The coordination number is four in square packing because there are four nearest neighbors.

The hexagon-based close packing shown in Figure 5.1 is ubiquitous in nature. In addition to the hexagonal packing of magnetic field lines dramatically illustrated by ferrofluids in Chapter 2, a bubble raft (a coalesced group of hundreds of bubbles) provides a simple, compelling illustration of nature's predilection for this packing arrangement. The bubble raft, like the optical transform experiment, is commonly credited to Sir Lawrence Bragg who developed it almost 50 years ago (*1*), though modern dishwashing detergent has supplanted Bragg's detailed formula for the medium supporting bubble formation in the raft. A diagram of the bubble raft setup is shown in Figure 5.2.

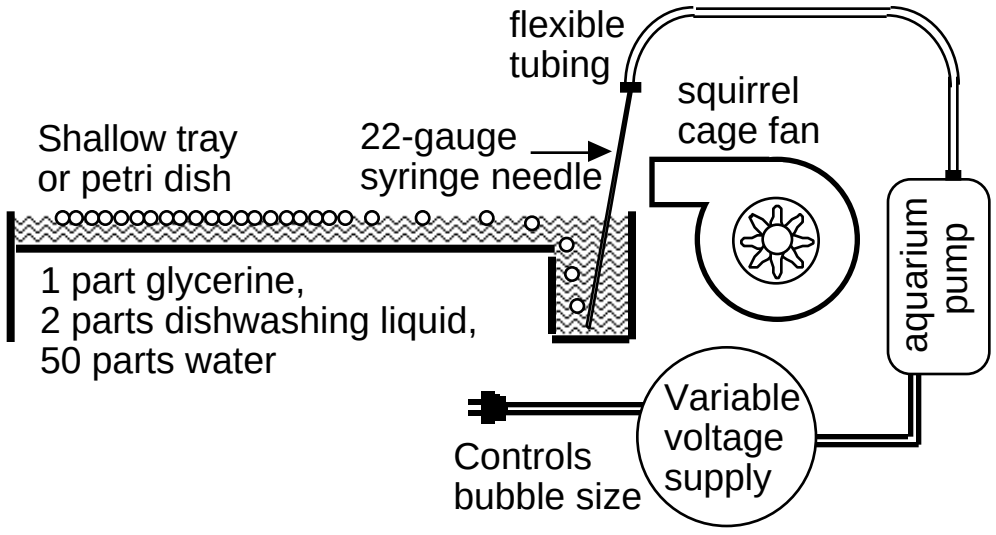

Figure 5.2. A diagram of a bubble raft.

The bubble raft provides an excellent two-dimensional model of a metal on the atomic level; the attraction of small bubbles for one another mimics the attractions between metal atoms in a crystal, bubbles of uniform size correspond to atoms, and the nondirectional forces that make the bubbles stick together correspond to the metallic bonding. The hexagonal arrangement of bubbles is the closest possible packing of bubbles and is caused by surface tension in the bubble raft.

Demonstration 5.1. Demonstrations of Close Packing: Bubble Rafts, BB Trays, and Bubble Wrap

Materials

Bubble raft apparatus—*see* Figure 5.2 (Its construction is shown in Appendix 5.3)
Bubble raft tray
22-gauge syringe needle
Aquarium pump (Hartz, for example)
Variable-voltage transformer
Flexible tubing
Small electric fan (optional)
Bubble solution made of 1 part glycerine, 2 parts thick commercial dishwashing detergent (Joy or Dawn work well), and 50 parts of water *(2)*
Overhead projector and screen

Procedure

- Fill the shallow tray to a depth of about 0.5 cm with bubble solution. For classroom demonstrations place the tray on an overhead projector. The tray design also helps protect the projection plate B (Appendix 5.3) from being scratched in use and storage.
- Connect a 22-gauge syringe needle (with the pointed tip ground off to prevent accidental skin puncture) to the hose (Tygon tubing) from an aquarium pump that is powered by a variable-voltage supply. Place the end of the needle under the surface of the bubble solution and adjust the voltage to produce small, uniform bubbles. (For a 4-W Hartz pump, 20 V works well.) Production of bubbles well below the solution surface in the deep end of the tray gives good bubble uniformity, but a better projection image is obtained through the shallow end.
- To aid in formation of the raft of bubbles, aim a small electric fan over the surface of the solution so that the bubbles are blown to the other end of the tray where they will begin to form the raft. Push aside unwanted bubbles with a Plexiglas slider (shown in Appendix 5.3) or scoop them out. To produce bubbles of uniform size, it is important to keep the needle near the bottom of the tray.

- Once the bubble raft has formed, turn off the aquarium pump and fan. The hexagonal arrangement of bubbles that occurs throughout much of the raft can be observed. Figure 5.3 shows a sketch of a typical raft. Defects in the regular hexagonal pattern are also generally observable and will be discussed in more detail in Chapter 6.

Variations

There are several variants of the bubble raft. A Petri dish works adequately, but the tray designed by Bragg, fabricated from Plexiglas, enhances the quality of the demonstration. Sealing metal BB pellets of uniform size in a plastic tray permits the BBs to be repeatedly shaken and will produce close packing that can be shown by laying the tray on an overhead projector. A detailed description of the construction of this tray is available.[3] Also available for projection on the overhead projector is the bubble wrap commonly used for packing; the bubbles in this plastic wrapping material form a close-packed array. The hexagonal packing arrangement can equivalently be modeled by placing seven identical coins or marbles on an overhead projector.

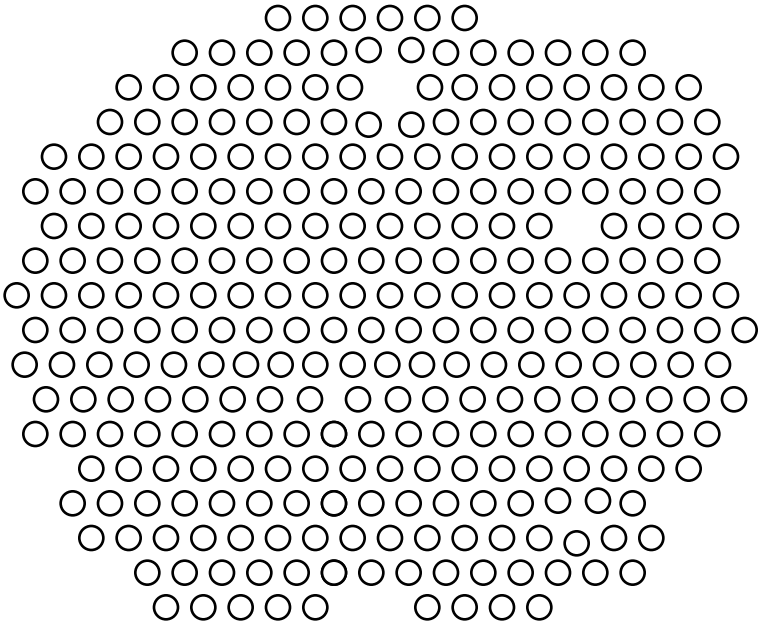

Figure 5.3. A typical bubble raft obtained using the setup shown in Figure 5.2.

[3]Assembly instructions for the BB board model are available from the Institute for Chemical Education.

Packing in Three Dimensions

If the spheres composing a square-packing layer (Figure 5.1B) are placed directly on top of one another, the simple cubic crystal structure♦ results (Figure 3.9). This structure is rare (Figure 3.11 shows the packing arrangements of the elements) and is characterized by low atomic density and coordination number. The density reflects the packing efficiency, defined in three dimensions as

$$\frac{\text{volume of spheres in the unit cell}}{\text{volume of unit cell}} \times 100\% = \%\ \text{packing efficiency} \qquad (2)$$

The packing efficiency of the simple cubic structure is only ~52%. The coordination number in this structure is six, with the nearest neighbors of any sphere defining the six corners of an octahedron, as partially shown in Figure 5.4.

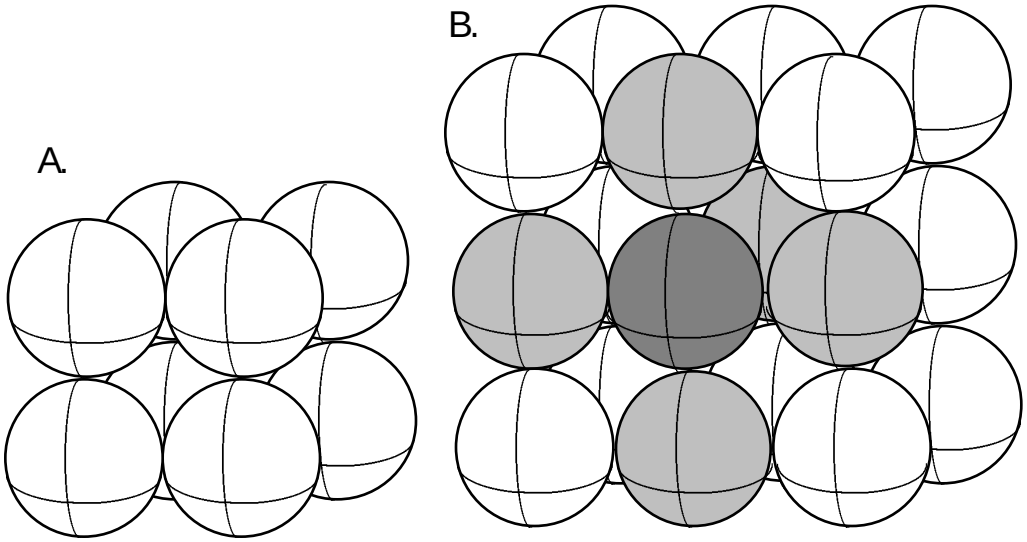

Figure 5.4. The simple cubic-packing arrangement showing (A) one unit cell, defined by the centers of the eight spheres that are shown; and (B) the octahedron of nearest neighbors (lightly shaded) around an arbitrarily selected atom (darker shading) in a simple cubic-packing array. (The sixth neighbor is in front of the page and has been omitted for clarity).

A more common packing arrangement results if the spheres in a square-packing layer are uniformly moved apart so they no longer touch, and the second layer is offset to nest in the spaces between the spheres in the first layer, as pictured in Figure 5.5A. The third layer and each succeeding odd-numbered layer is then in registry with the first layer; and the fourth and succeeding even-numbered layers are in registry with the second,

producing a more densely packed body-centered cubic structure♦ (Figure 3.10). In the bcc cubic unit cell the spheres touch only along body diagonals of the cube, as shown in the figure, and all layers are identical, but shifted relative to one another. The bcc packing efficiency is ~68%. Inspection of the structure reveals that the coordination number in the body-centered cubic structure is eight, with the nearest neighbors surrounding any given atom sitting at the corners of a cube.

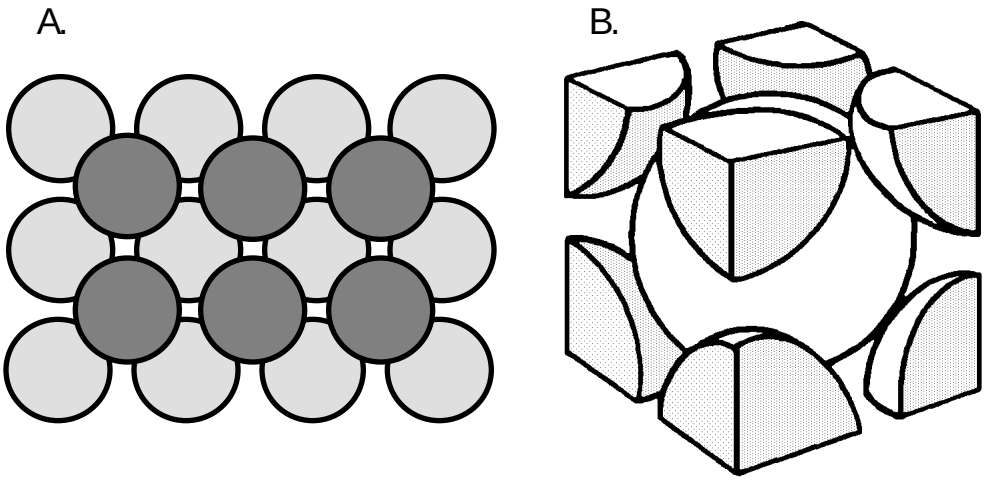

Figure 5.5. The body-centered cubic-packing arrangement. A: The shaded atoms are not touching and form a square-packed layer. The dark atoms form a second layer that is identical in arrangement to the first but shifted so that the atoms sit in the depressions formed by the first layer. The third, fifth, and subsequent odd-numbered layers are in registry with the first, while the fourth, sixth, and subsequent even-numbered layers are in registry with the second. B: A unit cell showing a central atom and its eight nearest neighbors. The latter are centered on the corners of a cube, and one-eighth of each of their volumes lies within the unit cell.

The two most dense three-dimensional packing arrangements of atoms for the metallic elements are hexagonal close packed (hcp) and cubic close packed (ccp). When stacking two-dimensional close-packed layers like that shown in Figure 5.1A, an arbitrarily chosen initial layer can be denoted A. The next close-packed layer, layer B, is placed such that the spheres rest in the hollows of the first layer. If the third layer (and every subsequent odd-numbered layer) is stacked directly over the first layer (layer A), and the fourth (and every subsequent even-numbered layer) is stacked directly over the second layer (layer B), then an ABAB... stacking pattern is formed, defining hexagonal close-packing (hcp) .

The coordination number in the hcp structure♦ (*see* Figure 5.6) is 12—a central sphere is touched by six spheres in its close-packed plane; by three in the close-packed plane above it; and by three more in the close-packed plane below it. The hcp structure has a packing efficiency of ~74%.

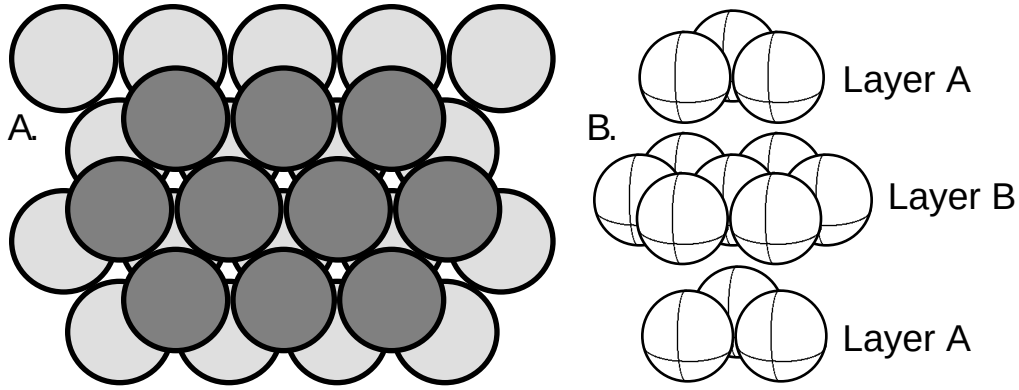

Figure 5.6. The hexagonal close-packed arrangement. A: A second hexagonal close-packed layer is resting in the depressions between atoms in the first close-packed layer. All odd-numbered layers are identical to the first, and all even-numbered layers are identical to the second. B: A second view of the hcp arrangement showing the ABAB packing of the close-packed layers.

Instead of placing the third close-packed layer directly above the first layer, layer A, it can be uniquely positioned to produce layer C, as sketched in Figure 5.7. The structure is then repeated with the fourth layer over the first, the fifth layer over the second, and the sixth over the third, leading to an ABCABC... structure that is called cubic close-packing (ccp)♦. The distinction between hcp and ccp is subtle (the same kind of close-packed layers are stacked but in different sequences), and several metals adopt both structures under different conditions.

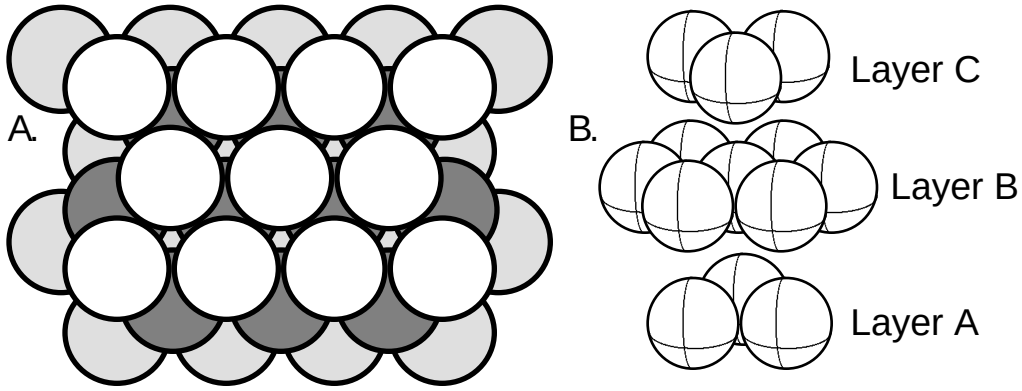

Figure 5.7. The cubic close-packed arrangement. A: The first two layers are identical to those in the hcp arrangement. The third close-packed layer rests in the depressions created by the second layer but in such a way that it does not match the first layer (*see* Figure 5.8). The fourth layer matches the first, the fifth matches the second, the sixth matches the third, and so on. B: A second view of the ccp arrangement that shows the ABCABC... arrangement of the layers.

Demonstration 5.2. Interstices in Close-Packed Structures

Materials

Overhead projector and screen
Thirteen identical coins
Magic markers
Figure 5.8 reproduced on a transparency (optional)
Bubble wrap and Ping-Pong balls (optional)

Procedure

- Arrange seven or more identical coins to form a close-packed layer on a blank transparency placed on the stage of an overhead projector.
- Label the interstices with B and C using a magic marker as shown in Figure 5.8 , or simply give the interstices different colors.
- Cover the interstices labeled B by a second layer of three coins. The interstices labeled C will still be visible. Place a third layer of coins over the original layer to form an hcp structure, in which case the interstices labeled C will still be visible. Alternatively, place the third layer over the interstices labeled C to form a ccp structure, in which case no interstices will be visible.

Variation

Bubble-wrap packing material with 1-inch-diameter bubbles can be placed on the overhead projector and Ping-Pong balls can be used to cover one set or another of the interstices.

The ABCABC packing arrangement is equivalent to the face-centered cubic structure (*see* Figure 3.12). This is readily seen with the SSMK: Two colors (or labels of any sort) are used to distinguish two types of principal spheres to show that a face-centered cube, standing on its body diagonal (the cube is upright on a corner), is camouflaged by the ccp structure, as shown in Figure 5.9A. In the fcc perspective♦ spheres touch along the face diagonals of the cube but not along the edges of the cube. Although the fcc and the ccp structure are equivalent, the close-packed planes in the fcc structure are those that are perpendicular to body diagonals of the cube. Because of the symmetry of the cubic unit cell, there are four such planes, sketched in Figure 5.9B.

The ccp and hcp structures differ only in the stacking sequence of close-packed planes; therefore, the packing efficiency (~74%) and coordination number (12) are identical.

Table 5.1 summarizes packing efficiencies and coordination numbers for the common structures described.

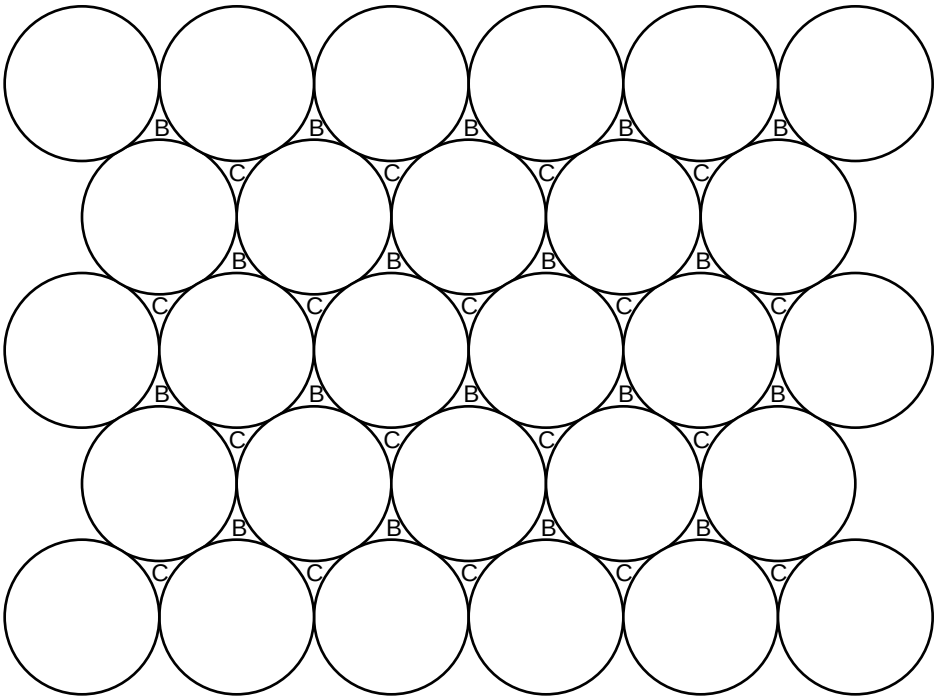

Figure 5.8. A close-packed array of spheres. Around any sphere there are six depressions or interstices labeled B and C that serve as possible resting sites for spheres in the next layer. However, only one set of interstices (set B or set C) can be filled with the next close-packed layer. If the spheres that make up the second layer are placed in the B positions, the C positions will still be visible (or vice versa). There are two ways of placing the spheres to form the third layer. If the spheres are placed so as to match the first layer (leaving the C interstices visible), ABAB... packing (hexagonal close packing) results. If the third layer is placed so as to occupy the C positions, ABCABC... packing (cubic close-packing) results.

Table 5.1. Packing in Metals

Type of Packing	Packing Efficiency[a]	Coordination Number
Simple cubic (sc)♦	52%	6
Body-centered cubic (bcc)♦	68%	8
Hexagonal close-packed (hcp)♦	74%	12
Cubic close-packed (ccp)♦ [b]	74%	12

[a]Measurement of the volumes of the cubic unit cells and the volumes of the spheres used to build the structures, for example with the SSMK, will allow an experimental determination of the packing efficiency that is in reasonably good agreement with these values.
[b]Identical to face-centered cubic (fcc).

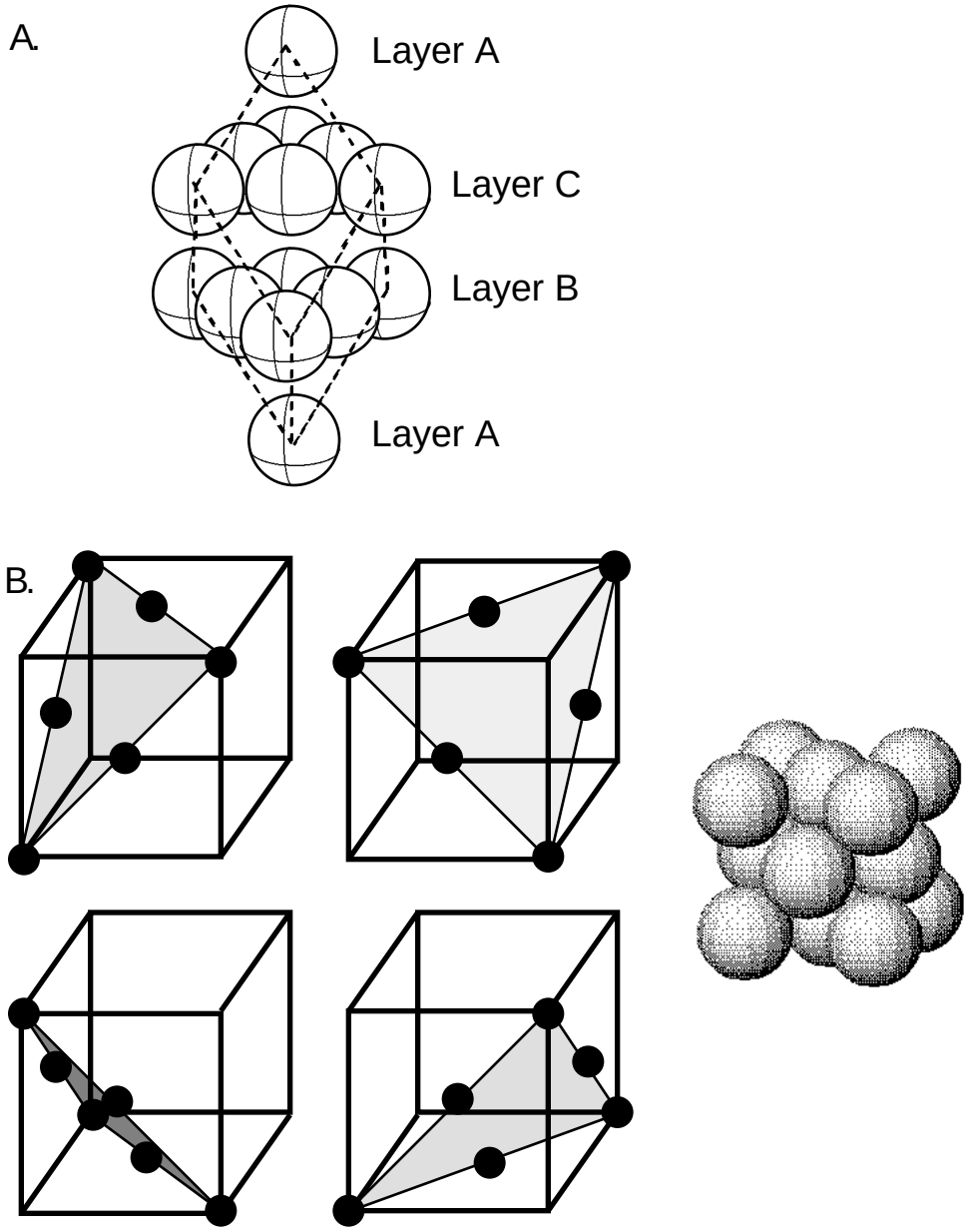

Figure 5.9. A: The cubic close-packed arrangement shown as a face-centered cube (dashed lines). Appropriate selection of one atom in the first and fourth layers and six atoms in each of the second and third layers generates a face-centered cubic unit cell. B: The close-packed layers are perpendicular to the body diagonals of the cubic unit cell.

Ionic Solids

The packing schemes described for metals serve as the basis for describing the structures of several important classes of ionic compounds. A general feature of many of the salts whose structures will be described is a framework comprising ions of one type, often the relatively large anions. These ions might be packed in a simple cubic (sc), hexagonal close-packed (hcp), or cubic close-packed (ccp) arrangement, perhaps "expanded" to move the like-charged ions farther apart from one another. The counterions needed for charge balance, often the smaller cations, are situated in holes or interstitial sites between the framework ions.

The size and shape of these holes reflect the geometry of the framework ions that form them. Holes derived from cubic, octahedral, and tetrahedral arrangements of packed anions figure prominently in describing extended structures. Using the hard-sphere model with the spheres in contact, the size of each of these holes can be calculated relative to the size of the spheres forming it. If the radius of the hole-forming spheres is taken as 1.000, the cubic, octahedral, and tetrahedral holes will accommodate spheres with radii of 0.732, 0.414, and 0.225, respectively. These relative sizes, so-called "radius ratios," are shown in Figure 5.10 and are the basis for the four sizes of spheres used in the SSMK. Furthermore, the SSMK can be used to build cubic, octahedral, and tetrahedral arrangements of spheres to investigate the relative sizes of the holes. The radius ratios are summarized in Table 5.2.

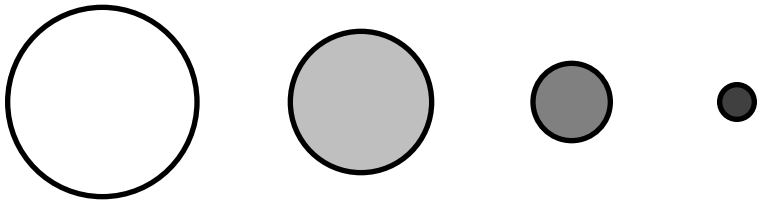

Figure 5.10. The radius ratio. The largest sphere is taken as the size of the close-packed anions and is arbitrarily given a radius of 1.000. The following three spheres can be accommodated in holes formed by arranging the large spheres in the shape of a cube (hole of radius 0.732), an octahedron (hole of radius 0.414), and a tetrahedron (a hole of radius 0.225).

Table 5.2. Radius Ratio Rules

Radius Ratio	Coordination Number	Type of Hole for Cation
0.225–0.414	4	tetrahedral
0.414–0.732	6	octahedral
0.732–1.000	8	cubic

The radius ratio serves as a rough guide to predicting what kind of hole the counterions will occupy.[4] For example, if the cation-to-anion radius ratio is slightly greater than 0.414, the cation should fit in an octahedral hole, representing a cation coordination number of six. As this ratio rises, there is more space around the cations. When the ratio reaches 0.732, there is enough space for eight anions around the cation, and cubic holes are often observed. If the ratio shrinks to below 0.414, the anions are too crowded relative to the smaller cation in an octahedral geometry; their repulsions can be reduced by a smaller coordination number and hole, favoring tetrahedral holes with the cation coordination number of four until a ratio of 0.225 is reached. [If the ratio becomes smaller than 0.225, even the low coordination number of four becomes unfavorable; a molecular analogy is that the thermal instability of tetraiodomethane, CI_4 , has been ascribed to the small ratio of the carbon-to-iodine radii *(6)*.]

Tetrahedral and octahedral geometries are commonly discussed in connection with molecular geometry and bonding in, for example, presentations of valence-shell electron-pair repulsion (VSEPR) rules and hybrid orbitals. Seeing these shapes in the different context of being "holes" in a framework provides a complementary spatial perspective, while underscoring the prevalence of these shapes in nature. Moreover, although the following structures are illustrated with salts, these same packing arrangements are encountered in metal alloys and molecule-derived (molecular) solids.

---

[4]The radius ratio is a simple and easily understood approximation for explaining the structures that are adopted by ionic compounds, but in many cases it makes the wrong predictions. Nathan (*3*) described 227 compounds and noted that the correct structural prediction is made for 67% of the compounds when the radius-ratio rule is applied. One contributing factor to the erroneous predictions is that the ions are not hard spheres, as assumed in the radius-ratio model, but have sizes that vary with the coordination number. (For example, sodium has an ionic radius that varies from a value of 1.13 Å in structures in which it is four-coordinate to 1.16 Å when six-coordinate, to 1.32 Å when eight-coordinate.) A second factor that causes deviation is that all bonds have some degree of covalency. As the amount of covalency increases, a hard-sphere (ionic) model will be less likely to describe the system accurately (*4*). Other schemes can be used to build structure-sorting diagrams that provide a basis for more reliable predictions, but with a resulting increase in complexity (*5*).

Demonstration 5.3. Models of Cubes, Octahedra, and Tetrahedra

Materials

Transparent dice (cubes)
Octahedra from inorganic model kits or some jacks (Many sets of jacks have one axis that is shorter than the other two.)
Tetrahedra from organic model kits
Octahedra and tetrahedra can be purchased separately in bulk quantities from Darling Models (see Supplier Information).
Paper models from Appendix 5.4
Mineral samples such as pyrite cubes (FeS_2) and fluorite octahedra (CaF_2), available from rock shops (optional)

Procedure

- Distribute the three shapes to each student or to groups of students so that they can examine the shapes while you discuss them.

Demonstration 5.4. Octahedral, Cubic, and Tetrahedral Crystals

Materials

Alum, $KAl(SO_4)_2 \cdot 12H_2O$
Sodium chlorate, $NaClO_3$
Borax, $Na_2B_4O_5(OH)_4 \cdot 8H_2O$
Water
Beakers, watch glass
Hot plate
Thread
Superglue (optional)

Procedure (based on recipes found in reference 7).

- To grow octahedral alum crystals, prepare a supersaturated solution by dissolving 20 g of $KAl(SO_4)_2 \cdot 12H_2O$ in 100 mL of H_2O. Heating will be necessary. When all the solid has dissolved, set the beaker aside in an area of constant temperature and cover with a watch glass. Crystals should appear in a few days, as they grow by slow evaporation.
- To grow cubic $NaClO_3$ crystals, use the same procedure, but dissolve 113.4 g of $NaClO_3$ in 100 mL of H_2O.
- To grow tetrahedral crystals, dissolve 113.4 g of $NaClO_3$ in 100 mL of H_2O. Add 6 g of borax to the solution. The borax is not incorporated into the $NaClO_3$ crystal but does affect the relative growth rate of the crystal faces. *See* Appendix 5.5.

- To grow larger crystals, you can "seed" a supersaturated solution. To prepare the seed, take a small crystal and attach it to a thread with a knot or a small drop of superglue. Prepare a supersaturated solution in which to place the seed. Once crystals begin to come out of the solution, suspend the seed crystal in the center of the solution. Be aware that the seed will dissolve if it is planted before crystals begin to appear. Cover the mixture and allow it to remain untouched and in constant temperature for a few days. Check the growth periodically.

Cubic Holes

Constructing a cubic unit cell with its corners at the centers of the anions in a sc packing arrangement of anions and placing a cation in its center yields a 1:1 cation-to-anion stoichiometry. Inspection of Figures 5.11 and 5.12 or comparison of the two CsCl structures in the SSMK♦ shows that this structure can also be described as comprising an anion in the center of a cube with a cation at each of the corners. From either perspective there is one cubic hole per framework sphere. This structure, which is often called the CsCl structure, can thus be regarded as two

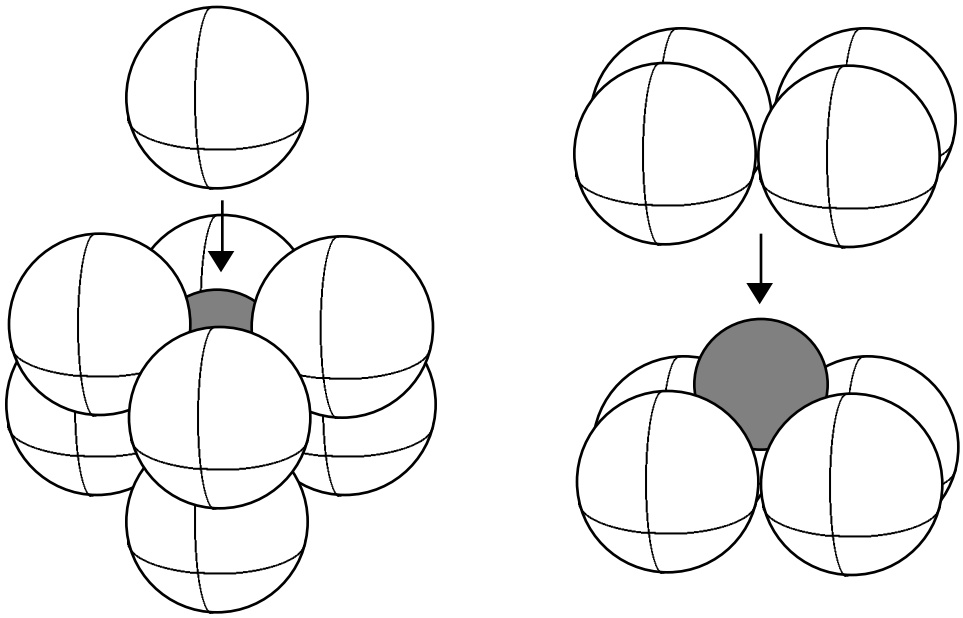

Figure 5.11. Two views of an atom (shaded sphere) in a cubic hole.

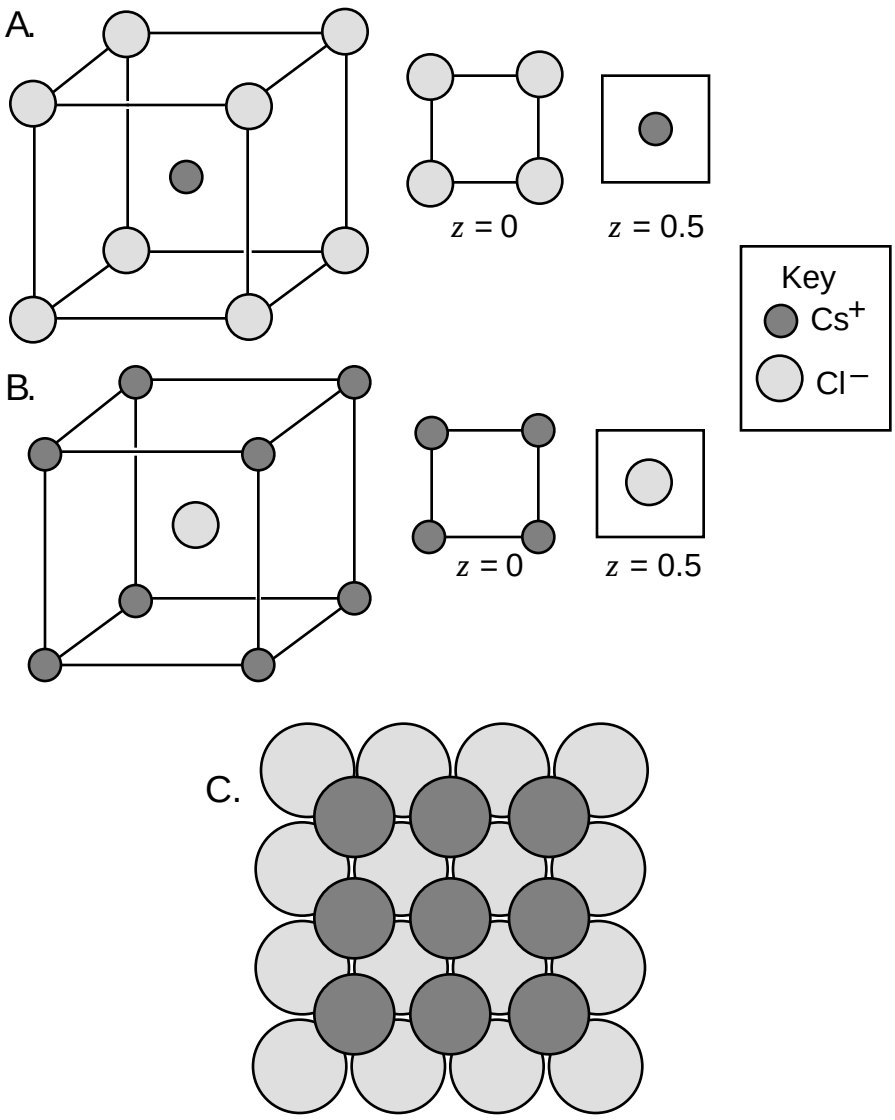

Figure 5.12. Three views of the CsCl structure. A: The cesium ion is in a cubic hole generated by chloride ions. B: Upon shifting origins the unit cell may also be viewed as having cesium ions at the corners of a cube and a chloride ion in the middle. C: A view of the alternating layers of square-packed cesium and chloride ions.

interpenetrating simple cubic frameworks.[5] This aspect of the structure is easier to see if a larger portion of the CsCl lattice is constructed♦. Cations occupy each cubic hole formed by anions; and anions occupy each cubic hole formed by cations. The coordination number of each anion and cation is eight. Both Cs^+ and Cl^- are about the same size, having radii of 1.69 and 1.81 Å, respectively. This same structure is adopted by the high-

[5]The CsCl structure is not body-centered cubic. A body-centered cubic structure has an identical environment at the corners and in the center of the unit cell. These environments are different in the CsCl structure.

temperature form of an alloy of NiTi, often called “memory metal” (Chapter 9). Other compounds that crystallize with the CsCl structure are listed in Appendix 5.6.

Octahedral Holes

The prototypical example of a structure featuring octahedral holes is the NaCl structure♦, the structure adopted by a large number of salts having 1:1 cation-to-anion ratios. In NaCl, where the ionic radii are 1.16 and 1.67 Å for Na^+ and Cl^-, respectively, the larger chloride ions may be viewed as sitting in ccp or fcc positions, forming octahedral holes, as shown in Figure 5.13. The structure emphasizing the fcc arrangement of Cl^- ions demonstrates that in the unit cell there is one octahedral hole for each close-packed Cl^- ion, which is filled by the smaller Na^+ ion. A total of four Cl^- ions are in the fcc positions of the unit cell (eight corner atoms times

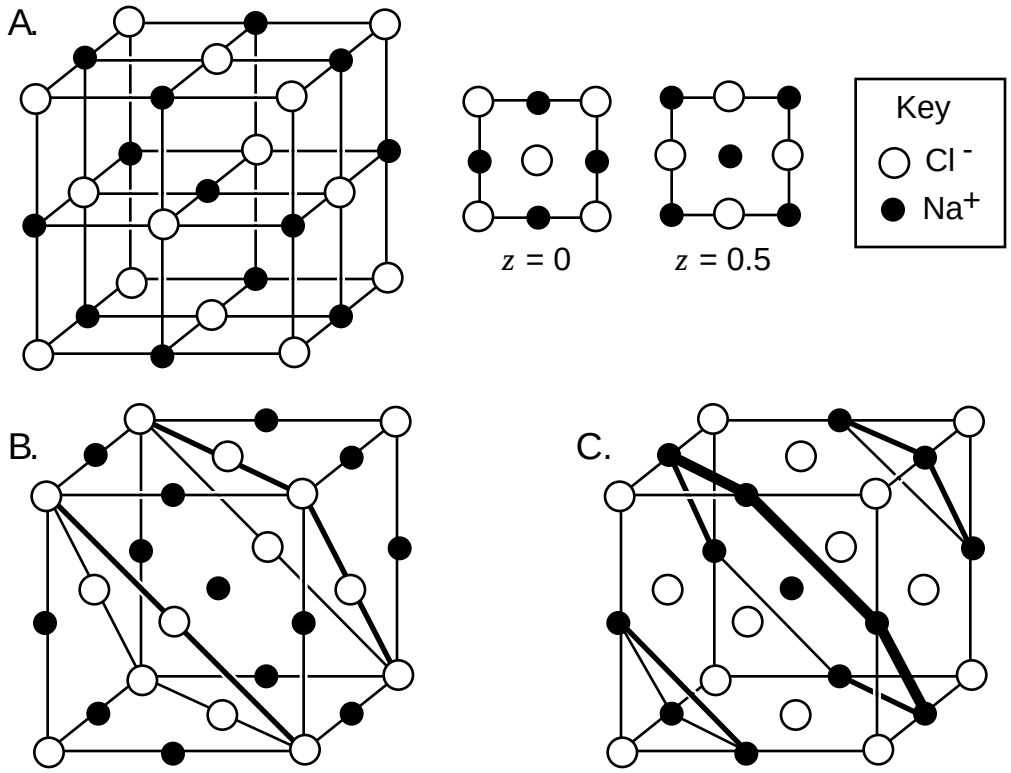

Figure 5.13. The NaCl structure. A: One unit cell of the NaCl structure in which the chloride ions may be viewed as forming a face-centered cubic arrangement with the sodium ions in the octahedral holes. B: A view of the unit cell in which the expanded close-packed planes of chloride ions are outlined. C: A view of the unit cell in which the expanded close packed planes of sodium ions are outlined. In B and C, these planes are perpendicular to a body diagonal of the cube (*see also* Figure 5.9).

1/8, plus six face-centered atoms times 1/2); one Na^+ ion is entirely within the unit cell; and 12 atoms are on the edges of faces of the unit cell (12 × 1/4 = 3), for a total of four. The unit cell thus corresponds to the formula Na_4Cl_4 or to the empirical formula NaCl. Although they are not close-packed, the Na^+ ions are packed in an expanded fcc geometry, with Cl^- ions filling all of the larger octahedral holes formed by the expanded arrangement of cations. This gives interpenetrating fcc arrangements of anions and cations, and each ion has a coordination number of six. Other compounds with the NaCl structure are listed in Appendix 5.6.

The octahedral hole is shown in isolation♦ in Figure 5.14. A view worth emphasizing is the creation of the octahedral hole by two triangular sets of spheres that arise from adjacent close-packing planes (the octahedron is resting on one of its faces that defines an equilateral triangle). The more conventional view of the octahedron resting on one of its vertices♦ is shown in Figure 5.14B.

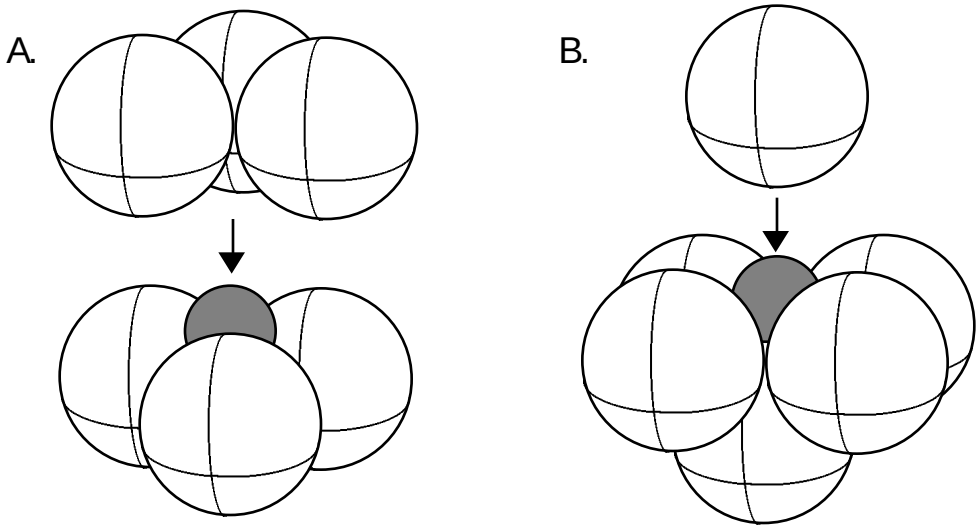

Figure 5.14. Two views of an octahedral hole. A: An octahedron resting on a triangular face. B: An octahedron resting on a vertex.

Fractional filling of octahedral holes also occurs. For example, with $CdCl_2$, the chloride ions are close packed, and only every other layer of octahedral holes (one-half of all such holes) is filled with the smaller Cd^{2+} ions♦, leading to the 1:2 cation-to-anion stoichiometry (*see* Figure 5.15). In this case, the coordination number of Cd^{2+} would still be six, but the coordination number of Cl^- would be taken as three, because each anion is surrounded only by three of the cations.

Since the packing of adjacent layers is identical in hcp and ccp structures, octahedral holes must arise in hcp packing, as well. The structures of NiAs♦ (Figure 5.16) and CdI_2♦ (Figure 5.17) illustrate complete filling and half filling of octahedral holes that result from hcp arrangements of As and I, respectively. Other solids that have these structures are listed in Appendix 5.6.

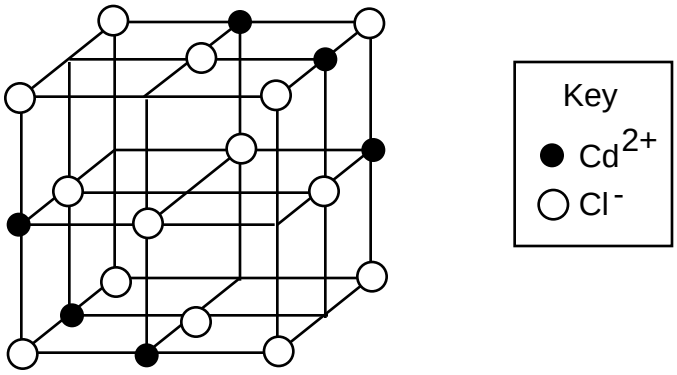

Figure 5.15. The $CdCl_2$ structure. This structure is generated by removing alternate planes of cations from the NaCl structure. The picture shown here does not represent a complete unit cell.

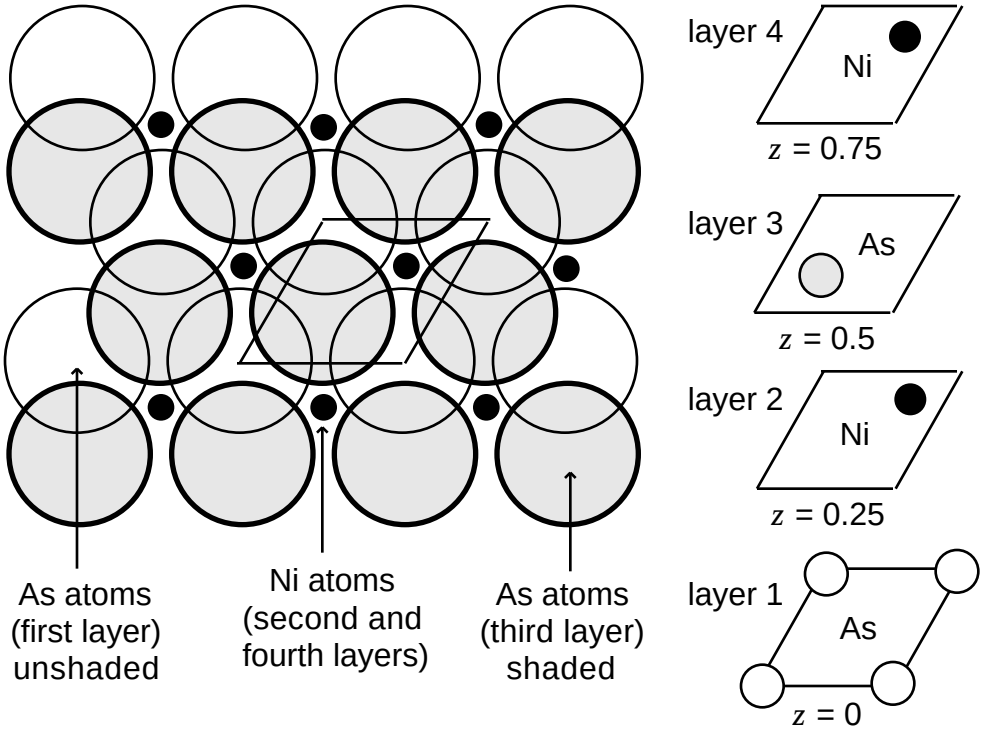

Figure 5.16. The NiAs structure. The arsenic atoms form a hexagonal close-packed arrangement (layers 1, 3, and layer 1 repeated are the ABA layers) while the nickel atoms occupy the octahedral holes. (The nickel atoms in layers 2 and 4 are in registry directly above each other and thus superimposed in the left view above.) The NiAs structure may be viewed as the hcp analog of the NaCl structure. There are two Ni atoms and two As atoms in the unit cell.

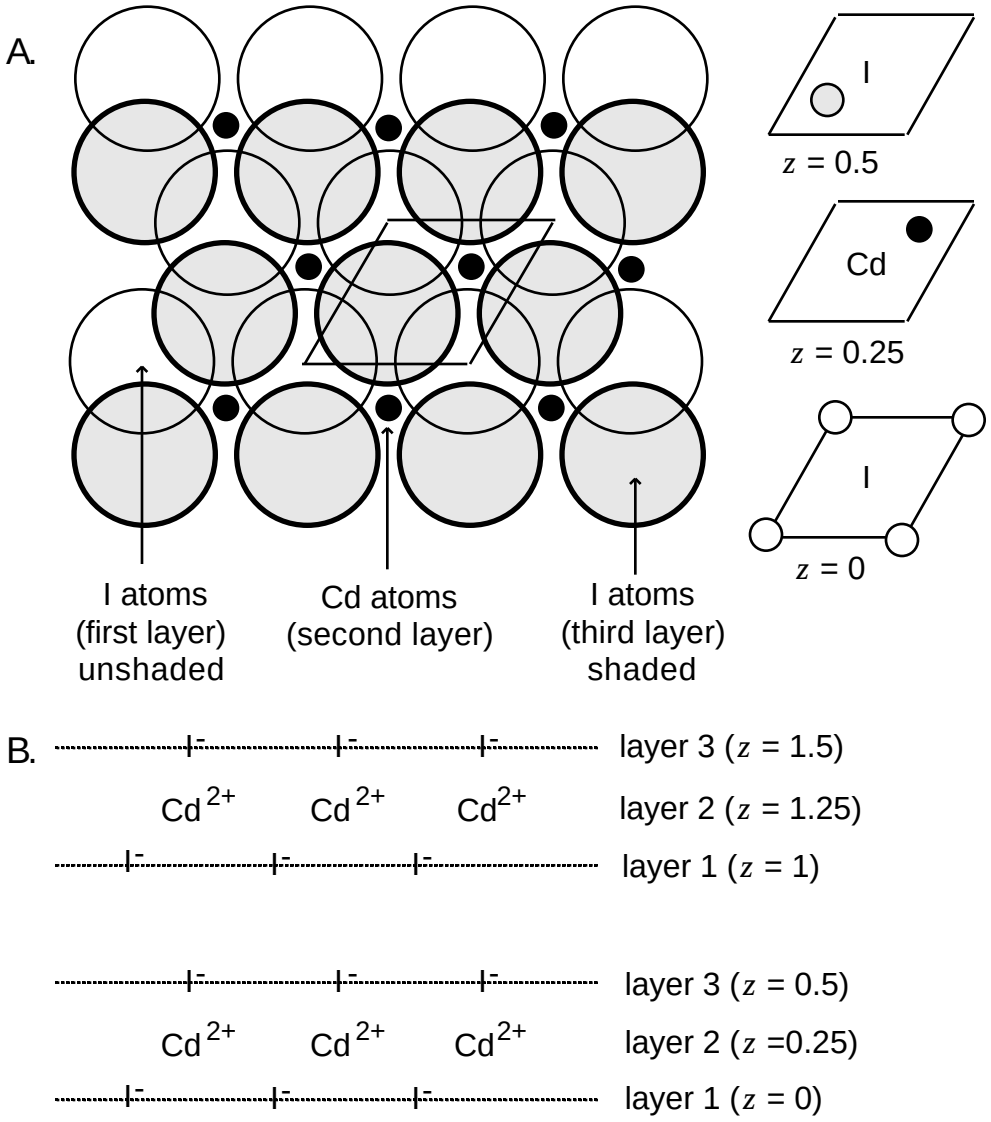

Figure 5.17. The CdI_2 structure. A: The iodine atoms form a hexagonal close-packed arrangement with the cadmium atoms in one-half of the octahedral holes (alternating planes of cations have been removed from the NiAs structure). B: A side view of the CdI_2 structure (this view is at 90° to the view shown in A) and the missing plane of Cd atoms (center). The CdI_2 structure may be viewed as the hcp analog of the $CdCl_2$ structure.

Tetrahedral Holes

As described earlier, tetrahedral holes resulting from close-packed spheres are relatively small. Figure 5.18 illustrates the formation of a tetrahedral hole both by capping an equilateral triangle of three close-packed spheres with a fourth, a view that emphasizes the formation of such holes between close-packed layers of spheres, and by placing two pairs of spheres perpendicular to one another.♦

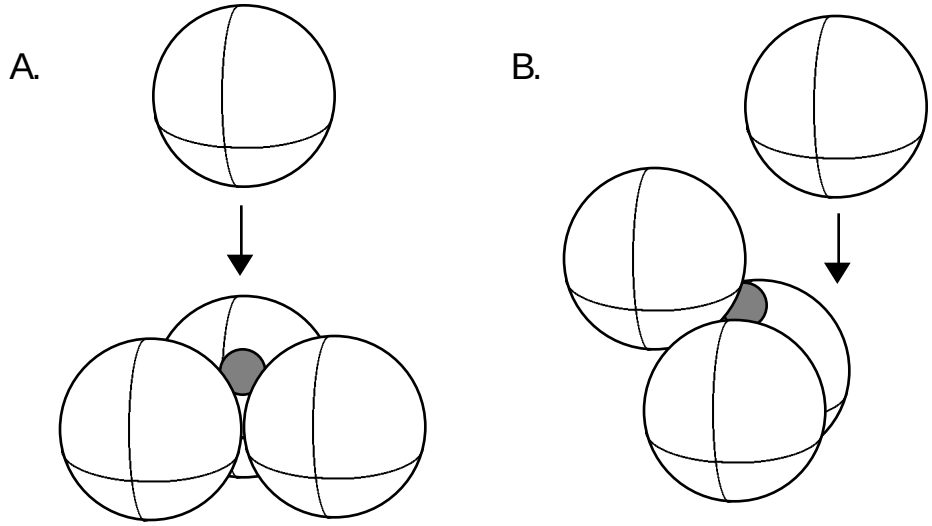

Figure 5.18. Two views of the tetrahedral hole. A: A tetrahedron generated by capping an equilateral triangle of spheres with a fourth sphere. B: A tetrahedron generated by two pairs of spheres with perpendicular orientations.

The antifluorite structure♦ (Figure 5.19) features dianions in an fcc (ccp) arrangement and monocations in all of the tetrahedral holes. This structure is adopted by Li_2O, for which the ionic radii are 0.73 and 1.28 Å for Li^+ and O^{2-}, respectively.[6] Inspection of the unit cell reveals that the four O^{2-} ions (eight corner atoms times 1/8, plus six face-shared atoms times 1/2) composing the fcc unit cell yield eight tetrahedral holes, all within the confines of the cell. There are thus two tetrahedral holes for each close-packed sphere, and in Li_2O they are all filled.

In fluorite, CaF_2♦, the positions of the cations and anions are reversed, as shown in Figure 5.20A. The Ca^{2+} ions are seen to lie in an "expanded"

[6]The radius ratio predicts octahedral coordination for Li^+, but there are not enough octahedral holes (one per oxygen) to match the required stoichiometry. Consequently, Li^+ fills all of the tetrahedral holes instead. This example reinforces the notion that the radius ratio is only a rough guide to predicting structure.

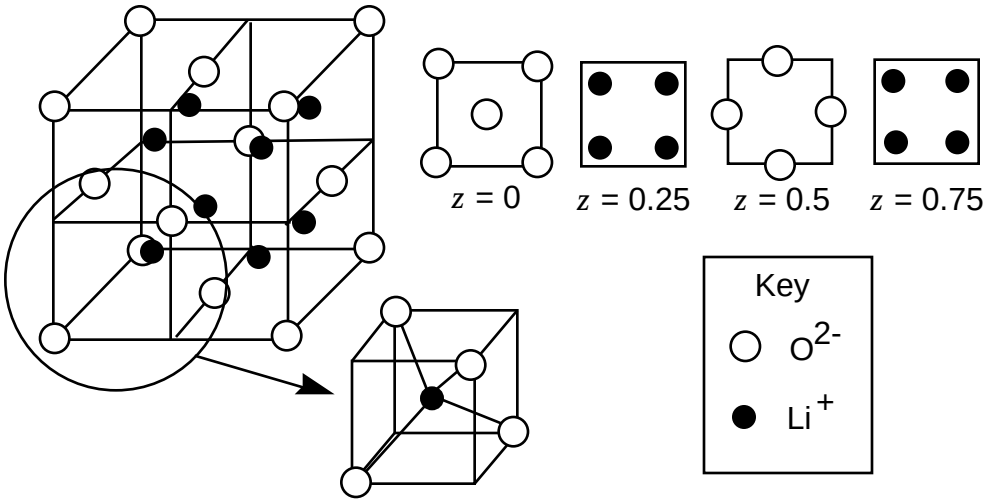

Figure 5.19. The Li_2O (antifluorite) structure. The oxygen atoms form an fcc array, and the lithium atoms occupy the eight tetrahedral holes in the unit cell. Expansion of the circled region shows the tetrahedral coordination of oxygen atoms about the lithium atom in one of the octants of the unit cell.

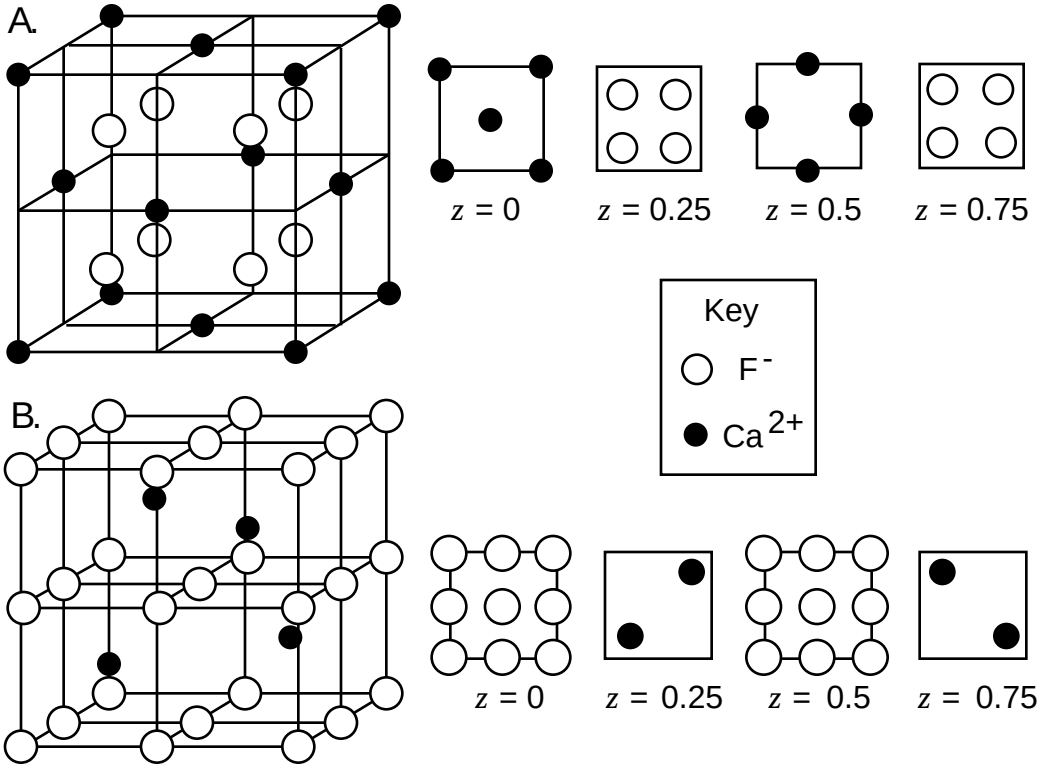

Figure 5.20. A: The CaF_2 (fluorite) structure. B: An alternate view of the CaF_2 structure in which the fluoride ions form a simple cubic arrangement with the calcium ions in half of the cubic holes.

face-centered cubic arrangement;[7] the intervening anions cause their internuclear separation to be a substantial 3.9 Å. This separation distance generates expanded tetrahedral holes for the F^- ions; again, all of the tetrahedral holes are filled, consistent with the 1:2 ion ratio in the salt.[8] Other compounds that have the fluorite or antifluorite structures are listed in Appendix 5.6.

The fluorite structure is also exhibited by a strikingly beautiful purple metallic alloy, $AuAl_2$, often dubbed the "purple plague." In the electronics industry, when Au and Al were sometimes used in close proximity on circuit boards, a purple color often appeared between strips of the two metals. (When the circuit board was used, it would become warm and cause the metals to diffuse and form $AuAl_2$. This alloy is conductive, so the circuit would short.) X-ray diffraction experiments and elemental analysis established the alloy to be $AuAl_2$, with the larger Au atoms (1.34 Å radius) in fcc positions and the smaller Al atoms (1.25 Å radius) in expanded tetrahedral holes.

Appendix 5.7 gives a procedure for preparing a sample of $AuAl_2$. The reactivity of this intermetallic compound provides an excellent illustration of the amphoteric character of aluminum: both acids and bases dissolve the aluminum from the $AuAl_2$, and thus permit the gold to be recovered essentially quantitatively.

Fractional filling of the small tetrahedral holes is illustrated by the important zinc blende structure, adopted by many common semiconductors (Chapter 7). In zinc blende (sphalerite)♦, a mineral form of ZnS, the larger sulfide ions (radius 1.70 Å) are found in a face-centered cubic arrangement similar to the oxide ions in antifluorite. In this case the small Zn^{2+} ions (radius 0.74 Å) are located in exactly half of the tetrahedral holes. The unit cell is shown in Figure 5.21. The Zn^{2+} ions themselves define an expanded tetrahedral hole for the sulfide ions, giving each ion a coordination number of four. The interpenetrating nature of the cations and anions allows each to produce a tetrahedral geometry. Other compounds that have the zinc blende structure are listed in Appendix 5.6.

The mineral wurtzite also has the formula ZnS♦. It differs from zinc blende in that the sulfide ions are now in an hcp rather than a ccp (fcc) arrangement (*see* Figure 5.22). But again, each ion is surrounded by four counterions in a tetrahedral geometry. Other compounds that have the wurtzite structure are listed in Appendix 5.6.

---

[7]Even though CaF_2 has a cubic unit cell, it is often found as octahedral crystals (*see* Demonstration 5.4). External shapes of crystals reflect the relative growth rates of their atomic planes. The octahedral faces of CaF_2 can be related to its cubic unit cell. *See* Appendix 5.5.

[8]CaF_2 may also be viewed as a simple cubic lattice of fluoride ions with the calcium ions in half of the cubic holes. (*See* Figure 5.20B.) The coordination number of the Ca^{2+} ions is 8 and that of the F^- ions is 4 (with tetrahedral coordination). The related structure, antifluorite, may be treated in a similar way: The SSMK shows different views that reveal large anions in fcc positions and small cations in expanded sc positions. Again, half of the cubic holes, now formed by the small cations, are filled by anions, yielding the same overall stoichiometry.

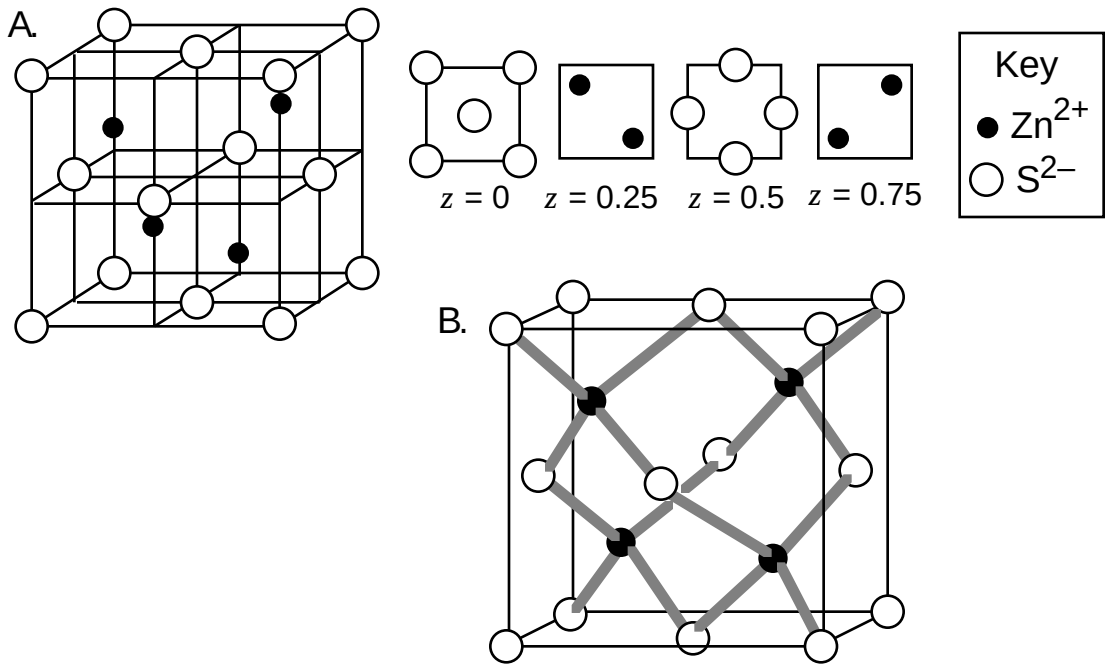

Figure 5.21. The zinc blende (sphalerite) structure. A: A view of the sphalerite structure showing that the sulfur atoms form a face-centered cubic arrangement with the zinc atoms in half of the tetrahedral holes. B: A view of the structure that emphasizes the tetrahedral coordination of the Zn atoms.

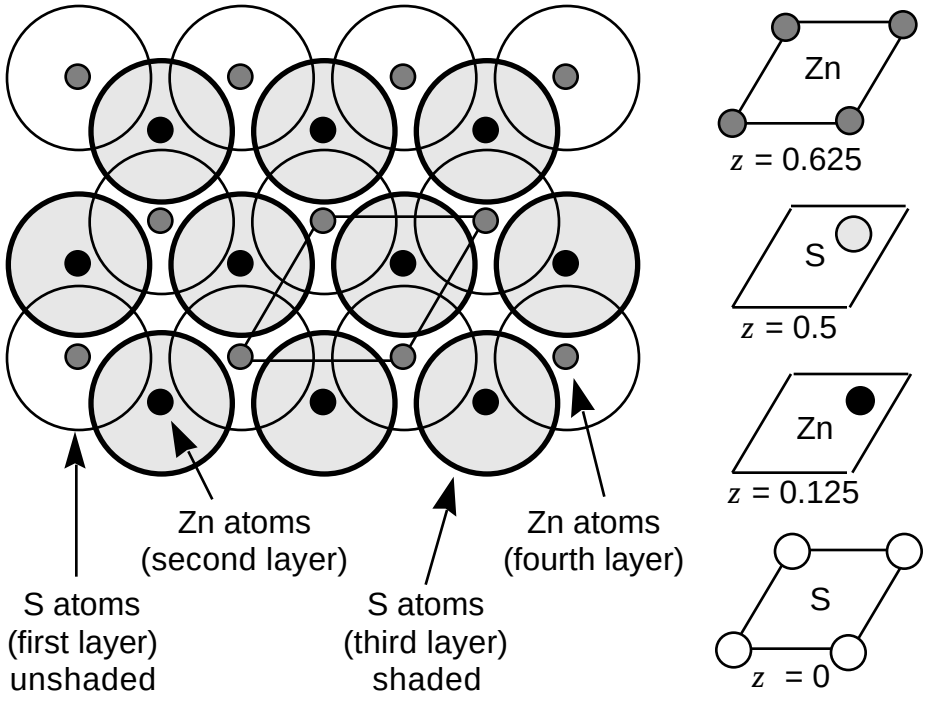

Figure 5.22. The wurtzite structure.

Sphalerite and wurtzite are polymorphic forms of zinc sulfide. In general, polymorphs are compounds (or in some cases, elements) that have the same ionic formulas or repeat units but exist in two or more crystalline phases, differing in atomic arrangement.[9]

Summary of Ionic Structures

In a close-packed structure, there are two tetrahedral holes and one octahedral hole per close-packed atom. The location of these holes is shown in Figure 5.23. Many structures are based on complete or partial occupancy of the tetrahedral or octahedral holes in close-packed arrays of atoms. This viewpoint provides a unifying approach to teaching the many structures that may initially seem unrelated. A summary of structures that can be described in this way is given in Table 5.3; structures that are based on the filling of cubic holes appear in Table 5.4.

Table 5.3. Structures Based on Close Packing of Anions, X

	Type of Close-Packing for X		Coordination Number	
Positions of Cations	ccp	hcp	M	X
All octahedral holes	$NaCl^{\blacklozenge}$	$NiAs^{\blacklozenge}$	6	6
Half of octahedral holes	$CdCl_2$[a]$^{\blacklozenge}$	CdI_2[a]$^{\blacklozenge}$	6	3
One-third octahedral holes	$CrCl_3$	BiI_3	6	2
All tetrahedral holes	Li_2O[b]$^{\blacklozenge}$	–	4	8
	CaF_2[c]$^{\blacklozenge}$	–	8	4
Half of tetrahedral holes	ZnS (zinc blende)$^{\blacklozenge}$	ZnS (wurtzite)$^{\blacklozenge}$	4	4

[a]Alternating planes of cations are removed (see Figure 5.15). In the case of $CdCl_2$, this corresponds to removal of layers of cadmium ions perpendicular to the body diagonal of the cubic unit cell.
[b]This is the antifluorite structure (anions ccp).
[c]This is the fluorite structure (cations ccp).
SOURCE: References 9 and 10.

Table 5.4. Structures Based on Simple Cubic Packing of Anions, X

		Coordination Number	
Position of Cations	Example	M	X
All cubic holes filled	$CsCl^{\blacklozenge}$	8	8
Half of cubic holes filled	CaF_2[a]$^{\blacklozenge}$	8	4
Half of cubic holes filled	Li_2O[b]$^{\blacklozenge}$	4	8

[a]This is an alternate way of viewing the fluorite structure (anions sc).
[b]This is an alternate way of viewing the antifluorite structure (cations sc).
SOURCE: References 9 and 10.

[9]Contrast polymorphs with allotropes, which are different forms of the same element. In this case the number of atoms in the formula units may be also different (e.g., O_2 and O_3). Reference 8 gives a further discussion of the distinction between polymorphs and allotropes.

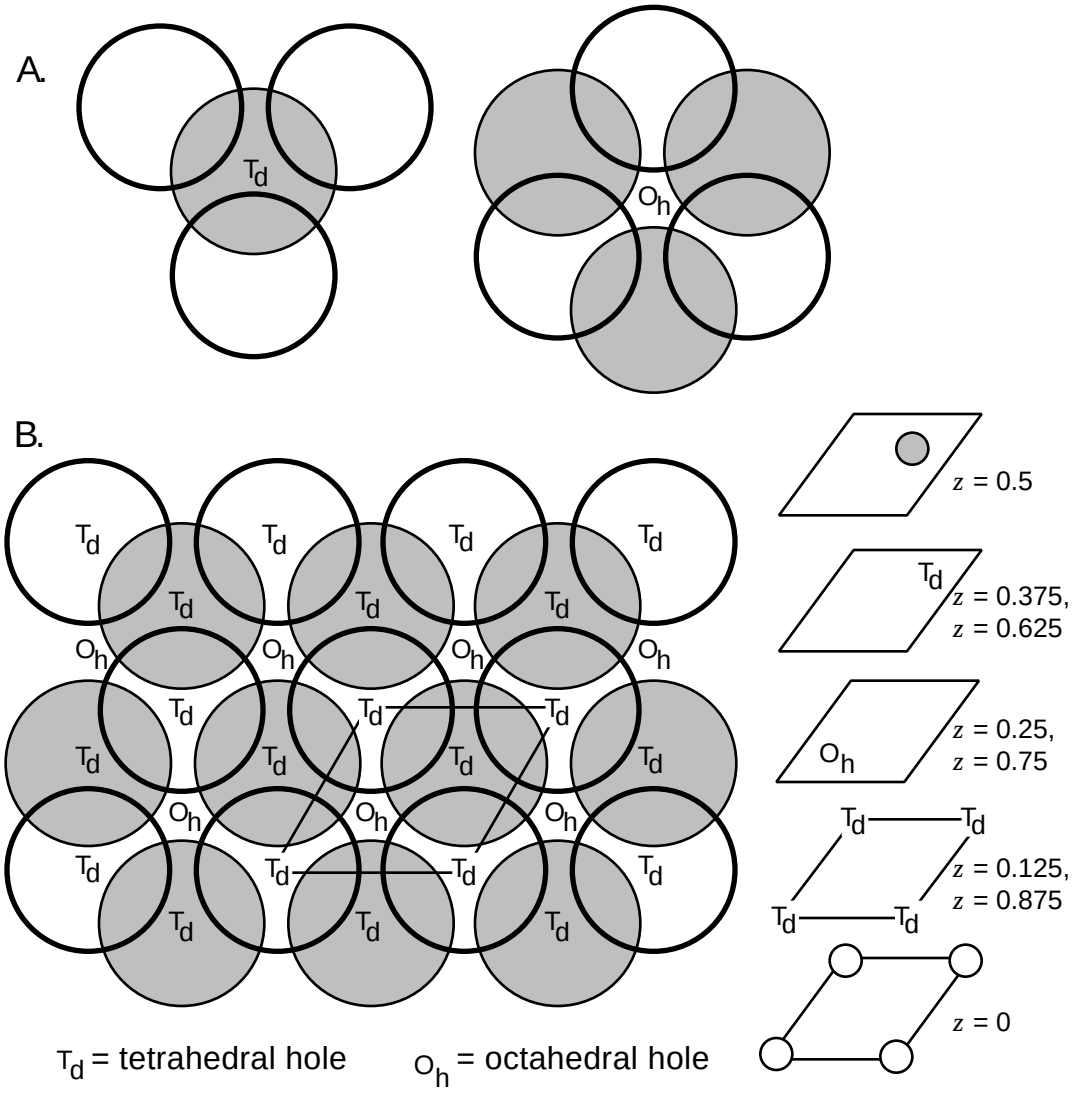

Figure 5.23. A: A tetrahedral hole, T_d, and an octahedral hole, O_h, shown in isolation (*see also* Figures 5.14 and 5.18). B: The first two close-packed layers of atoms in a hcp arrangement of atoms showing the location of octahedral and tetrahedral holes. A parallelogram that defines the base of a unit cell is superimposed. The *z*-layer diagrams for the unit cell show that there are two tetrahedral holes and one octahedral hole per close-packed atom. (Just as atoms on an edge of a unit cell count as contributing one-quarter of their volume to the unit cell, the tetrahedral holes on unit cell edges may be viewed as being one-quarter within a particular unit cell.) There are also two tetrahedral holes and one octahedral hole per atom in a fcc unit cell (*see* Figures 5.13 and 5.19).

Laboratory. Experiment 2 is a laboratory experiment that uses the SSMK to explore the structures of metals and ionic compounds. Topics such as packing efficiency, coordination number, and hole size are also covered.

Covalent Solids

In passing to covalent extended solids, directional bonding replaces the largely nondirectional bonding characteristic of metals and salts. The prototypical example of a covalently bonded solid is the diamond allotrope of carbon. The diamond structure is also exhibited by the elements silicon, germanium, and α-tin. Inspection of the cubic unit cell of the diamond structure♦ (Figure 5.24) reveals it to be a very open structure relative to those of metals and salts. The packing efficiency is, in fact, only about 37%, or about half that of the common metal structures. Each carbon atom is tetrahedrally bonded to four other carbon atoms. Eight atoms compose the unit cell: four are contained entirely within it. The other four are represented by the eight atoms at the corners of the cube and the six in the centers of the cube faces. A comparison with the zinc blende structure (Figure 5.21) demonstrates that the two structures are similar, the difference being that two kinds of atoms are used in zinc blende, with each atom tetrahedrally coordinated exclusively to the other kind of atom.

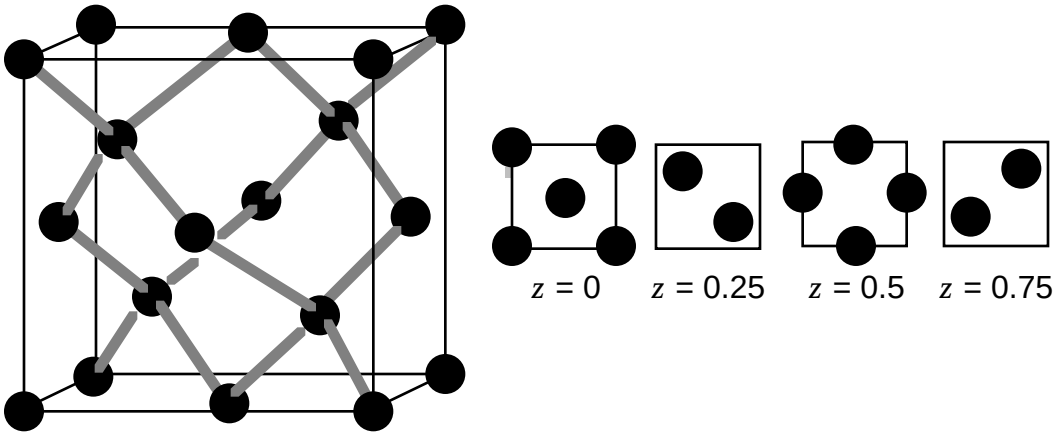

Figure 5.24. The diamond structure.

Another important allotrope of carbon is graphite. Unlike the structures described thus far, graphite's strong covalent bonds lie entirely within planes, making this a two-dimensional layered solid (*see* Figure 5.25). Construction of a model of the structure♦ shows that the spacing between layers (3.35 Å) is substantially larger than the interatomic distance within

layers of 1.42 Å. The coordination number of the carbon atoms is only three. Layers are held together primarily by weak van der Waals forces, permitting them to slide relative to one another. Graphite is a lubricant because of this property.

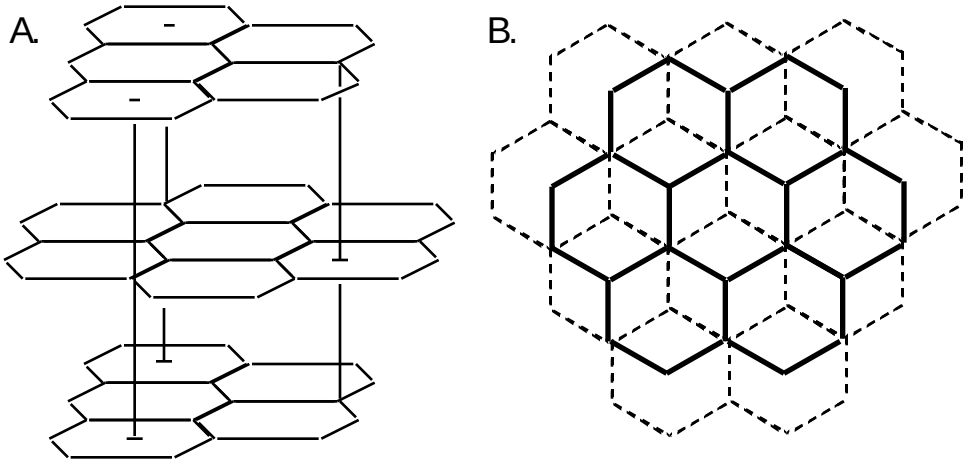

Figure 5.25. Two views of graphite. A: Side view of graphite showing the planar arrays of fused six-membered rings. The second layer is not aligned with the first; however, alternate layers are in registry. B: Top view of graphite showing how the second layer (dashed lines) is oriented with respect to the first layer (solid lines). Half of the atoms have another atom directly below them, and the other half do not.

Another layered solid with a larger component of ionic bonding than graphite is the mineral molybdenite (molybdenum disulfide)♦. As shown in Figure 5.26, the coordination number of the molybdenum is six, defining a trigonal prismatic (one equilateral triangle directly above another) geometry; and that of sulfur is three, because sulfur atoms cap equilateral triangles of molybdenum atoms. The layers of sulfur atoms that do not sandwich molybdenum atoms are in contact with one another. The like-charged sulfide layers would be expected to repel one another; these layers are held together by weak van der Waals forces.

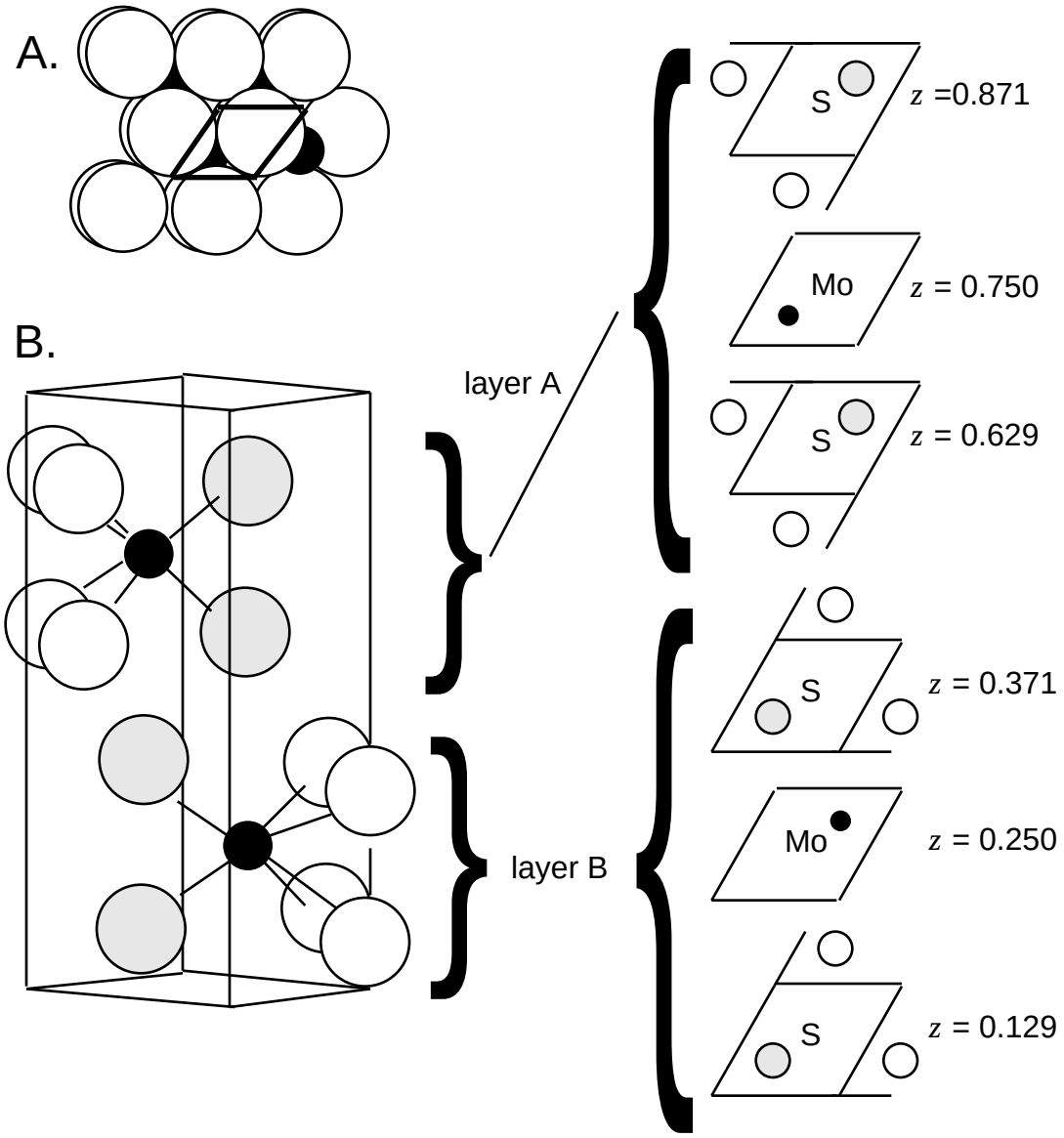

Figure 5.26. The molybdenum sulfide (MoS_2) structure. A: Top view. The structure may be viewed as consisting of pairs of eclipsed hexagonal arrays of sulfur atoms with molybdenum atoms in the trigonal prismatic holes. A unit cell is superimposed. B: Side view. The molybdenum atoms (black) and the shaded sulfur atoms are within the unit cell. The molybdenum atom in layer A is directly above the sulfur atoms in layer B, and the sulfur atoms in layer A are directly above the molybdenum atom in layer B. Layer A is attracted to layer B by weak van der Waals forces. The sulfur atoms in layer A are sitting in the depressions created by the hexagonal array of sulfur atoms in the adjacent layer. Consequently, alternate layers are in registry.

Demonstration 5.5. Removal of Graphite and Molybdenum Sulfide Layers

Materials

MoS_2 (Wards Natural Science, *see* Supplier Information) and/or graphite lumps
Transparent cellophane tape

Procedure

- Lightly press a piece of tape against a sample of MoS_2 or graphite and then remove it. Some layers of the solid will stick to the tape.
- As noted in the section on the STM (Chapter 2), the interlayer forces are sufficiently weak in these materials that a piece of tape can be used to lift off layers from them and reveal fresh surfaces.

Variations

- Students can perform this demonstration themselves if pieces of tape (or a tape dispenser) and samples of the solids are distributed throughout the class. Alternatively, pieces of tape with small amounts of the layered solid already attached can be lightly fastened to a rod or a yardstick for ease in distribution. Students can be asked to lightly fold the tape onto itself, which will transfer layers from one half of the tape to the other half.

Molecular Solids

The molecules in molecular crystals are often held together by weak van der Waals forces. Some of the same packing arrangements discussed earlier are used here, as well. For example, molecules of buckminsterfullerene, C_{60}, pack in the fcc arrangement in the solid state. This packing can be illustrated by simply building the fcc structure♦ with each sphere representing a C_{60} molecule. In K_3C_{60}, all of the octahedral and tetrahedral holes in the fcc arrangement of buckminsterfullerene anions are filled with potassium cations.

More Connections to Molecular Shapes: Extended Shared Polyhedra

The importance of the octahedron and tetrahedron in extended structures is underscored by the multitude of solids that can be constructed by sharing corners, edges (and occasionally faces) of these shapes. For example, isostructural solids like ReO_3 and idealized WO_3♦ can be described as consisting of MO_6 octahedra with the metal atom at the center and shared oxygen atoms at the corners, as sketched in Figure 5.27. The octahedra are combined to create an extended three-dimensional structure by corner-sharing each of the oxygen atoms between two octahedra. The cubic unit cell corresponds to a chemical formula of MO_3, because only one quarter of each oxygen atom belongs to any given unit cell. Coordination numbers for the metal and oxygen atoms are six and two, respectively.

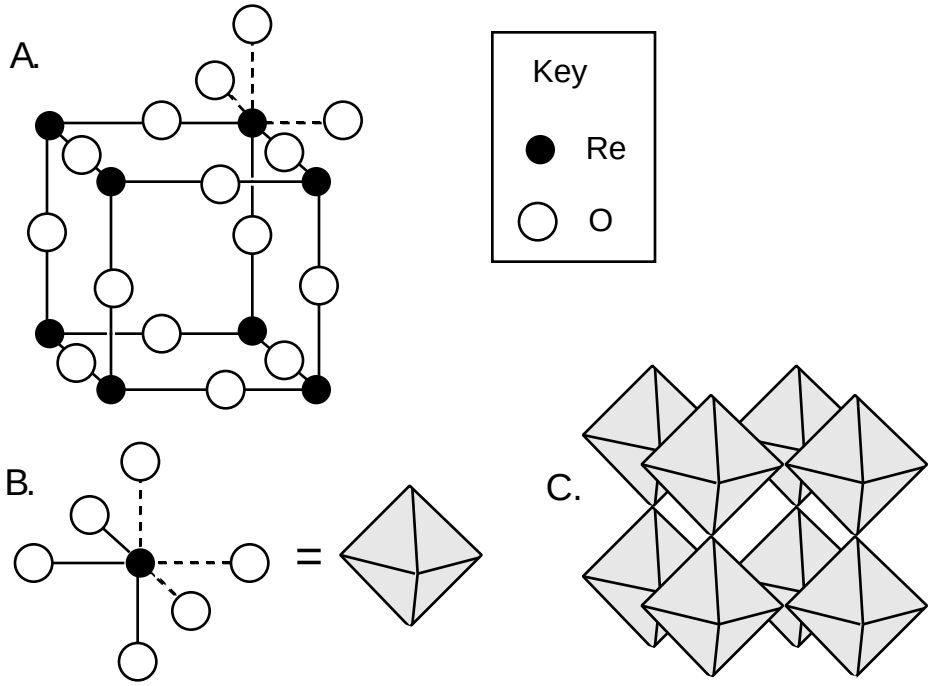

Figure 5.27. Representation of structures by octahedra. A: The ReO_3 unit cell; the dashed lines represent completion of one octahedron of oxygen atoms about a given Re atom. B: Replacement of the ReO_6 coordination sphere with an octahedron. C: The ReO_3 unit cell represented as a series of corner-shared octahedra.

Similarly, the perovskite structure♦ features corner-shared TiO_6 octahedra, with Ca^{2+} ions at the corners of the cubic unit cells in which the octahedra are inscribed, leading to the formula $CaTiO_3$ (*see* Figure 5.28A and 5.28B). A shift in origin that places the larger Ca^{2+} cations at the

center of the cubic unit cell leads to another common representation of the structure (Figure 5.28C and 5.28D). Coordination numbers of the calcium, titanium, and oxygen atoms are 12, 6, and 2 (or 6, including contacts of oxygen to both metals), respectively. Among the important examples of related perovskite structures are high-temperature superconductors (Chapters 1 and 9). The sequence shown in Figures 5.29 and 5.30 illustrates how the idealized perovskite structure is altered to produce the superconducting $YBa_2Cu_3O_7$ phase.

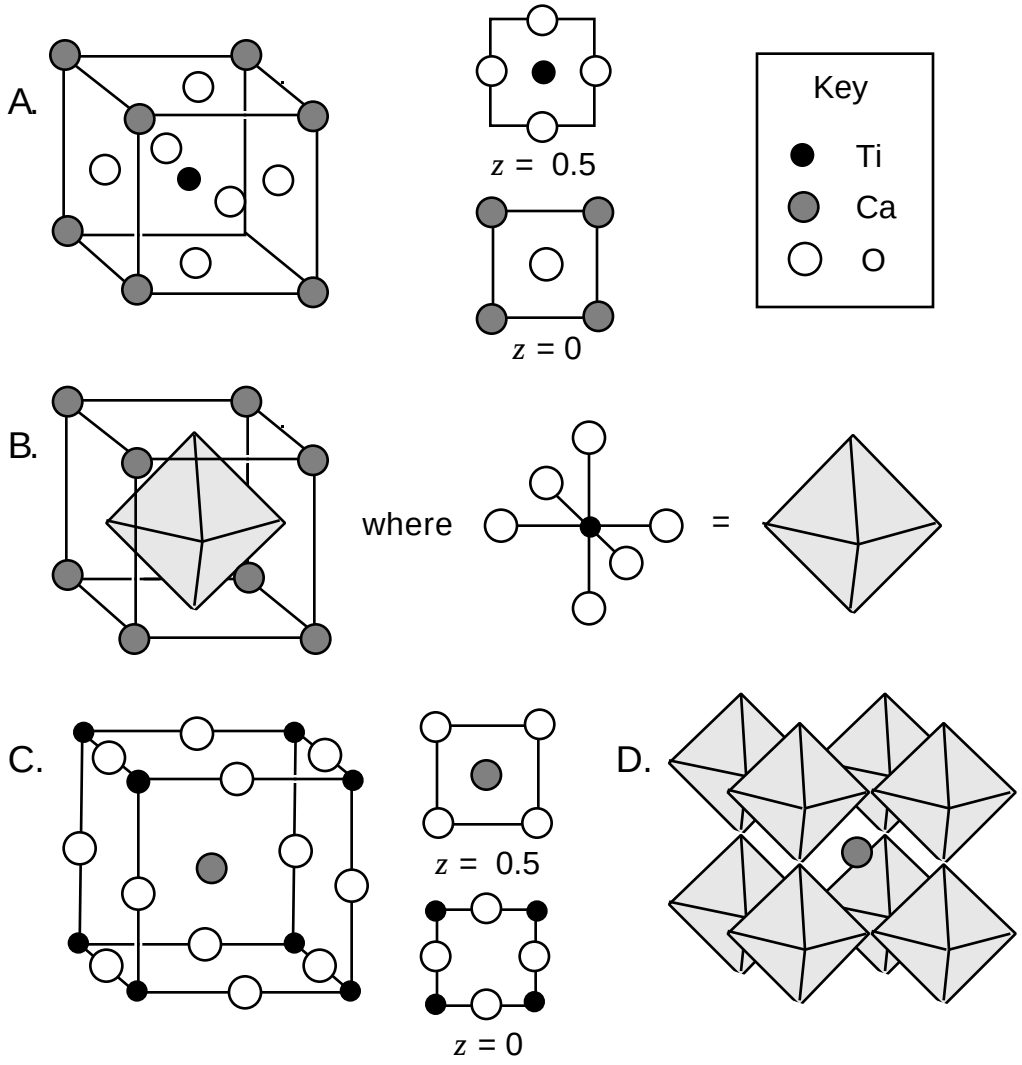

Figure 5.28. The perovskite structure. A: A unit cell with titanium at the center. B: The same unit cell showing the octahedral arrangement of oxygen atoms around a titanium atom. C: Shift in the unit cell to place calcium in the center. D: The unit cell shown in C represented as a set of corner-shared TiO_6 octahedra.

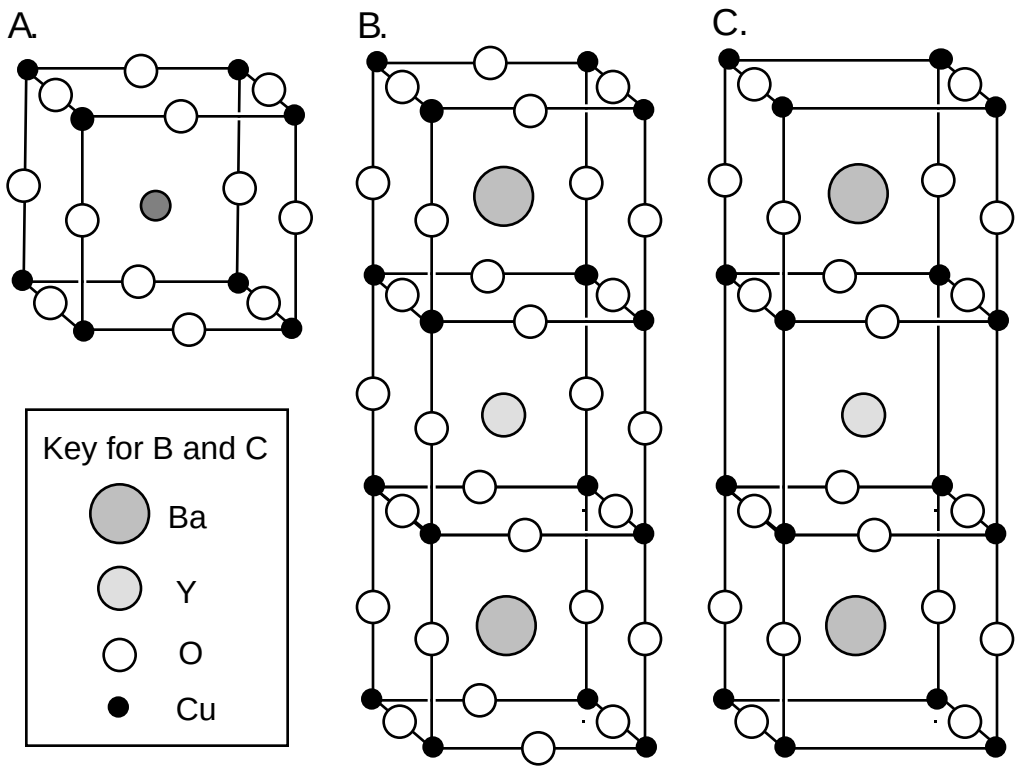

Figure 5.29. Construction of the $YBa_2Cu_3O_7$ superconductor by stepwise alteration of the perovskite structure. A: The perovskite structure as depicted in Figure 5.28C. B: Stacking of three perovskite unit cells followed by replacement of the calcium atoms by barium atoms in the first and third unit cells and by yttrium atoms in the second. In addition, copper is now in the titanium positions. This yields an idealized stoichiometry of $YBa_2Cu_3O_9$. C: Removal of eight edge-shared oxygen atoms (for a total of two oxygen atoms removed) to generate the idealized structure of $YBa_2Cu_3O_7$.

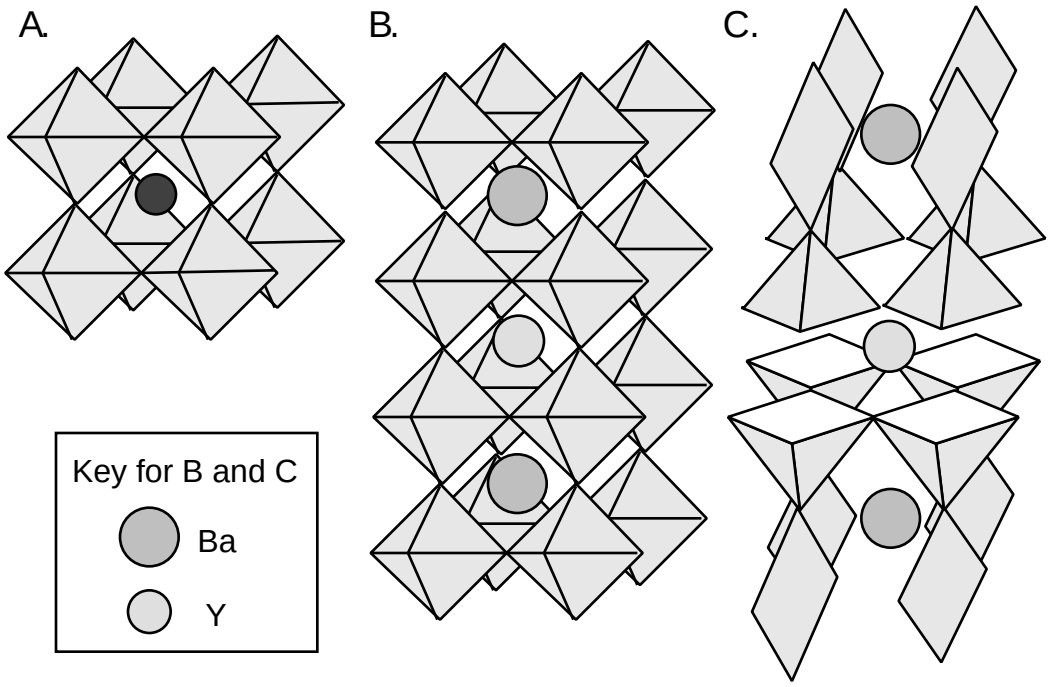

Figure 5.30. Representation of the construction of the $YBa_2Cu_3O_7$ superconductor as a series of fused octahedra. The steps are identical to those described in Figure 5.29. Removal of oxygen atoms in C converts the octahedra to square pyramids and squares.

Like octahedra, tetrahedra can be corner-shared. The most common structures based on linked tetrahedra are undoubtedly those of the silicate minerals *(11)*. The basic building block is the SiO_4^{4-}, or silicate, ion (*see* Figure 5.31A). Though there is not a wide variety of examples, several common minerals contain the silicate anion. These include zircon, $ZrSiO_4$; the garnets, $[(M^{2+})_3(M^{3+})_2(SiO_4)_3]$ where $M^{2+} = Ca^{2+}$, Mg^{2+}, or Fe^{2+}, and $M^{3+} = Al^{3+}$, Cr^{3+}, or Fe^{3+}; and olivine, M_2SiO_4 where $M = Mg^{2+}$ or Fe^{2+}. Both garnet and olivine form extensive series of solid solutions (*see* Chapter 3 and Experiment 14), as a result of substitution at the cation sites.

Successive linking of oxygen atoms at one, two, three, or four vertices of the tetrahedron generates a wide variety of discrete ions, rings, chains, sheets, and three-dimensional structures. If two tetrahedra are linked through the sharing of an oxygen at a common vertex, the result is the disilicate ion, $Si_2O_7^{6-}$ (*see* Figure 5.31B). This ion is not common in nature, although the mineral thortveitite ($Sc_2Si_2O_7$) is one example.

If the silicate ion shares oxygen atoms at two vertices of the tetrahedron, rings or chains may be constructed. Cyclic silicates are known with three, four, six, and eight linked tetrahedra. The most well-known of these is the mineral beryl, which has the formula $[Be_3Al_2(Si_6O_{18})]$ and contains a cyclic array of six tetrahedra (*see* Figure 5.31C). Many examples of linear silicates are known, and minerals with this structural feature are known as pyroxenes. The formula for the silicate repeat unit is $(SiO_3^{2-})_n$ for a

pyroxene mineral. Examples include diopside ($CaMgSi_2O_6$) and spodumene ($LiAlSi_2O_6$), the most commercially significant lithium-containing ore.

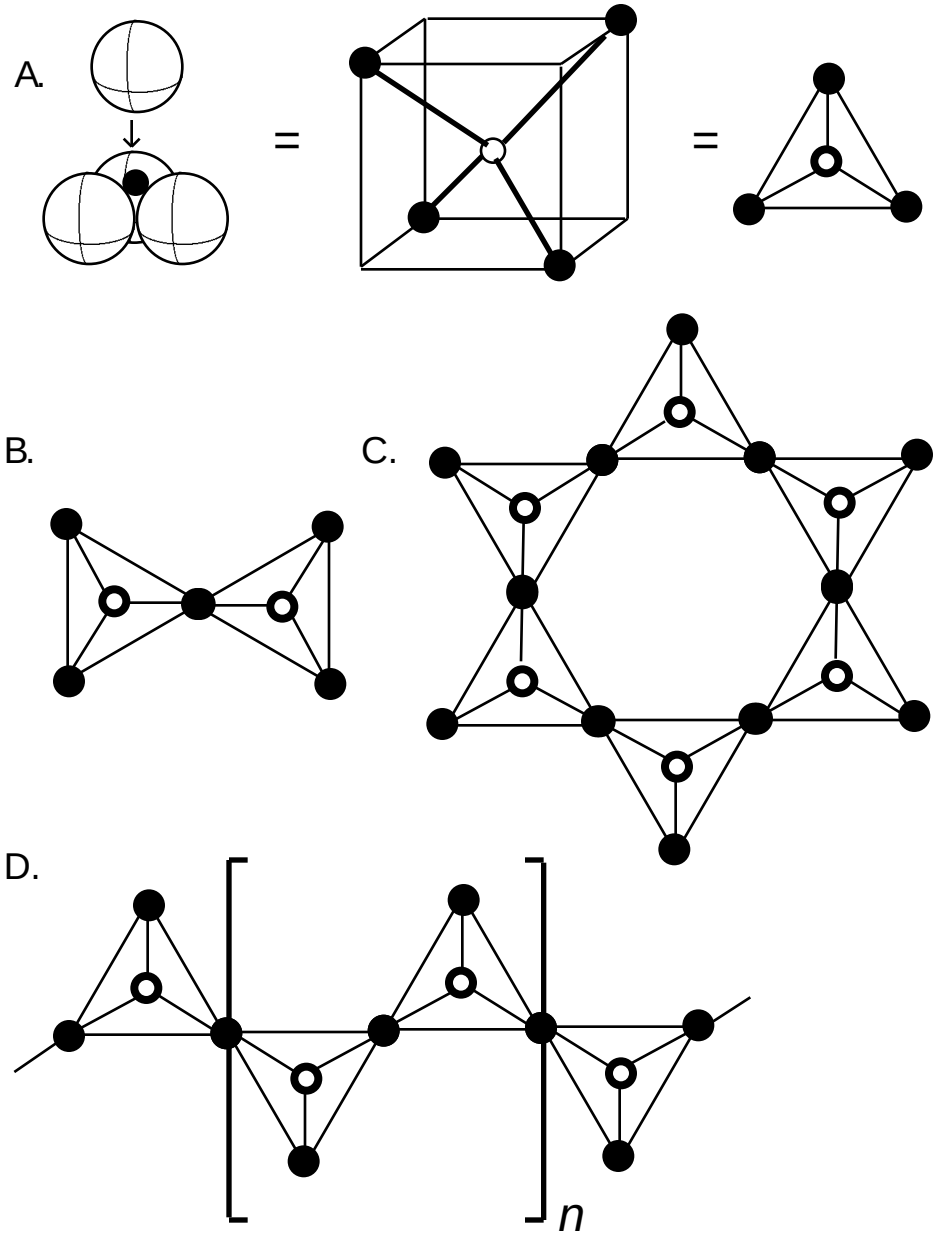

Figure 5.31. Silicate ions. A: Viewing the SiO_4^{4-} tetrahedron down one of the Si–O bonds generates the projection in which the oxygen atoms appear as black spheres at the vertices of a triangle and the silicon atom (white sphere) is below the fourth oxygen. B: The disilicate ion, $Si_2O_7^{6-}$. C: The cyclic $Si_6O_{18}^{12-}$ ion. D: A pyroxene shown without its cations. The silicate portion of the structure has the formula $(Si_2O_6^{4-})_n$.

If the linear chains are linked so as to form double chains with the repeat unit formula $(Si_4O_{11}^{6-})_n$, the series of minerals known as the amphiboles is generated. The silicate tetrahedra share two or three vertices of the tetrahedron (*see* Figure 5.32). A typical example is crocidolite, $Na_2(Fe^{2+})_3(Fe^{3+})_2(OH)_2(Si_4O_{11})_2$. This asbestos mineral has long been valued for its heat and fire resistance. It cleaves in the long thin fibers typical of asbestos, which have been found to constitute a health hazard.

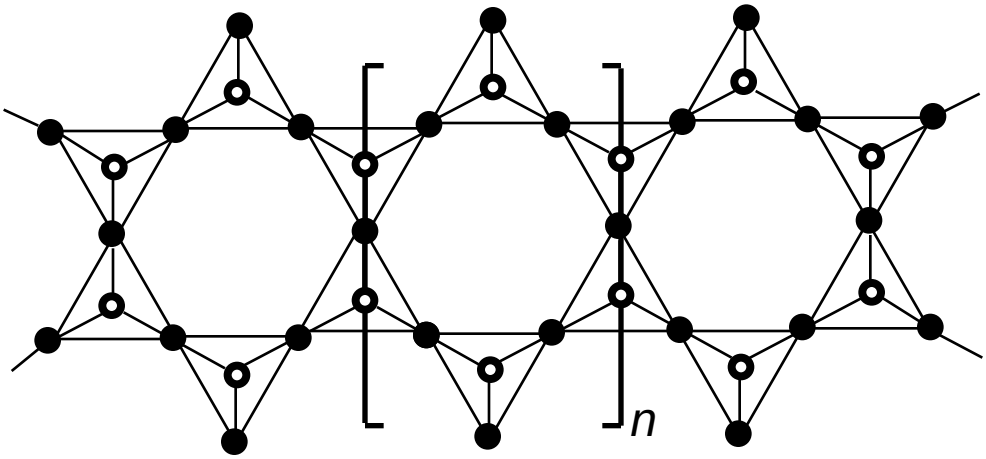

Figure 5.32. Fusing two chains into double chains forms the amphibole structure. The formula for the silicate chain is $(Si_4O_{11}^{6-})_n$.

If the side-to-side linking of chains is continued, a sheet-like structure is produced. The repeat unit for the silicate network is $(Si_2O_5^{2-})_n$ (*see* Figure 5.33). The minerals talc and mica have just such a structure (*see* Figure 5.34A). Its formula is $Mg_3(OH)_2(Si_4O_{10})$, and two parallel sheets actually have the unshared oxygen atoms of the tetrahedra pointing toward each other. In the middle of this sandwich are the magnesium and hydroxide ions, which serve to bind the two silicate layers together. Only van der Waals forces hold one pair of silicate sheets to the next. This feature accounts for the softness of talc.

An important feature of the silicate minerals is that aluminum may substitute for silicon in the tetrahedra. Because this is a formal replacement of Si^{4+} by Al^{3+}, the net charge on the structure must also change. This case is called isomorphous substitution if the structure does not change.

In the mica structure, one of every four silicon atoms is replaced by aluminum, and the formula for the aluminosilicate sheets becomes $AlSi_3O_{10}^{5-}$. These sheets can form a double layer similar to the talc structure. In the mica known as biotite, Mg^{2+} or Fe^{2+}, together with hydroxides, act to hold the sheets together, generating the formula $[(Fe,Mg)_3(OH)_2(AlSi_3O_{10})]^-$. The parentheses around Fe and Mg indicate that they form a solid solution (*see* Chapter 3). A mineral sample may have three iron atoms per formula unit or three magnesium atoms per formula

unit (or any combination of the two that adds up to three, including fractional values) and still be classified as biotite.

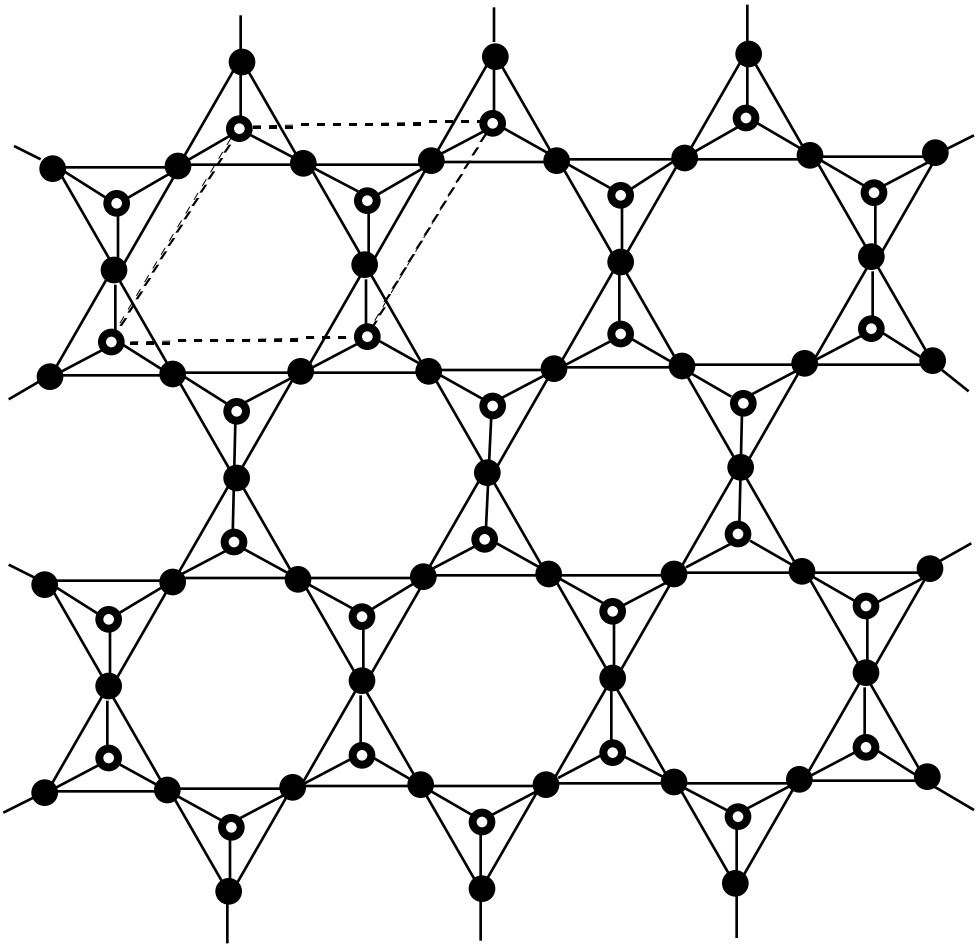

Figure 5.33. Fusing of the double chains forms two-dimensional sheets. The silicate portion of the structure has the formula $(Si_2O_5^{2-})_n$. The dashed lines represent a repeat unit for the sheets.

The exchange of Al^{3+} for Si^{4+} has created an excess of one unit of negative charge per substitution. Electroneutrality requires the addition of a monocation such as K^+, which is located outside the double layers. The presence of the potassium ions helps to hold the double layers to each other and serves to make mica harder than talc (*see* Figure 5.34). However, cleavage still occurs between the double layers. The mineral muscovite $[KAl_2(OH)_2(AlSi_3O_{10})]$ has a structure that is similar to biotite. The clay minerals such as fuller's earth, china clay (kaolin), and vermiculite (a common packing material) also have layered structures.

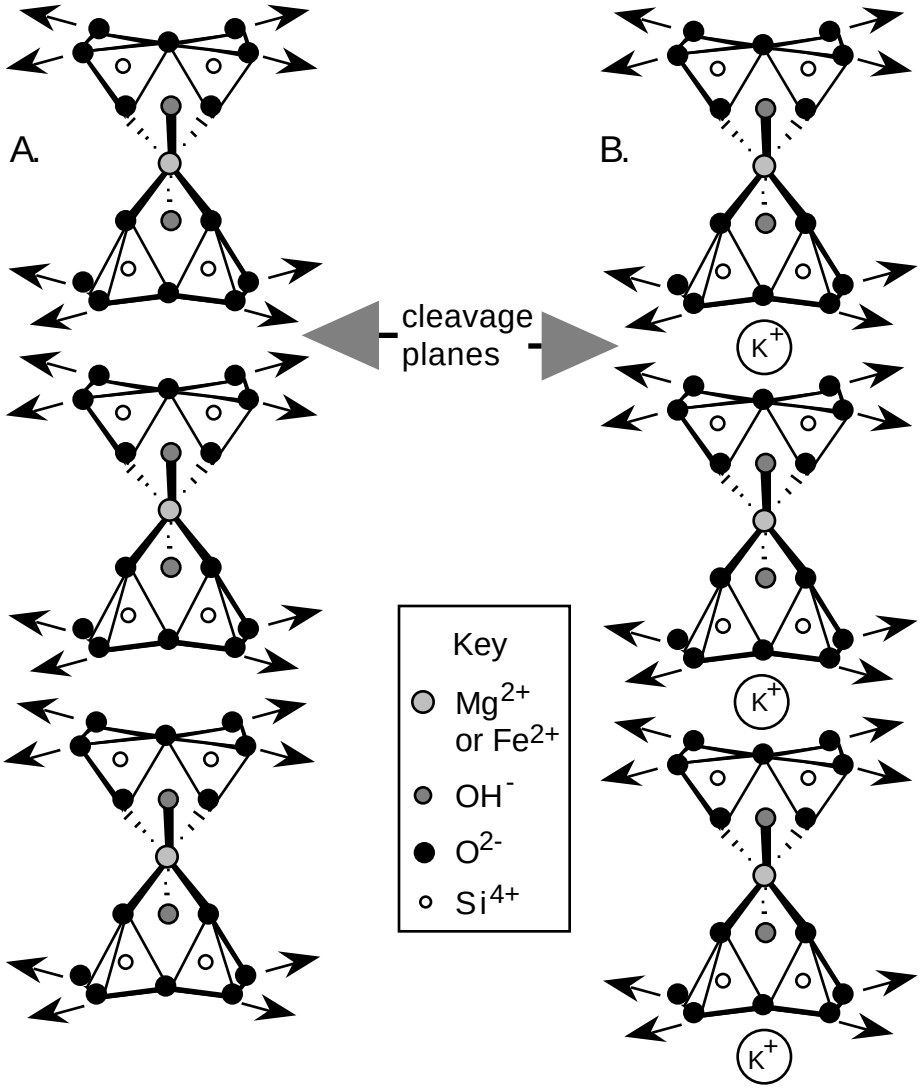

Figure 5.34. A cross-sectional view of the structures of talc and mica. The tetrahedra are portions of sheets as shown in Figure 5.33. The silicate sheets are all parallel, occur in double layer pairs with the unlinked oxygen atoms oriented toward each other, and continue in the direction of the arrows. A: The talc structure. The negatively charged sheets are held together by mutual attraction to a layer of magnesium ions in between. Weak van der Waals forces hold each pair of sheets to the next. B: The biotite mica structure. Replacement of one of every four silicon atoms by aluminum atoms in the sheets creates the need for additional positive charge in order to maintain electrical neutrality. These cations (potassium in biotite) are located outside of the double layer that contains the magnesium ions. Thus they serve to hold one layer to the next. In both cases cleavage involves separation of one double layer from the next.

Laboratory. The use of X-ray diffraction to measure the repeat distance in the stacking direction for layered materials, including these layered silicates, is described in Experiment 5.

Continued linking of silicate or aluminosilicate structures can result in the formation of complex frameworks that contain pores or channels that are large enough for water, small molecules, or cations to fit inside. Such materials are called zeolites (*see* Figures 5.35 and 5.36). They have been used to remove water from organic solvents (molecular sieves), to exchange sodium ions for calcium or magnesium ions in water softeners, and to prepare synthetic gasoline from such feedstocks as methanol. In the latter case, a zeolite catalyst called ZSM–5 was developed by Mobil and is believed to involve sites of high Lewis acidity that activate the methanol toward carbon–carbon bond formation. This catalyst is also shape-selective, permitting only molecules of certain sizes to migrate through the channels.

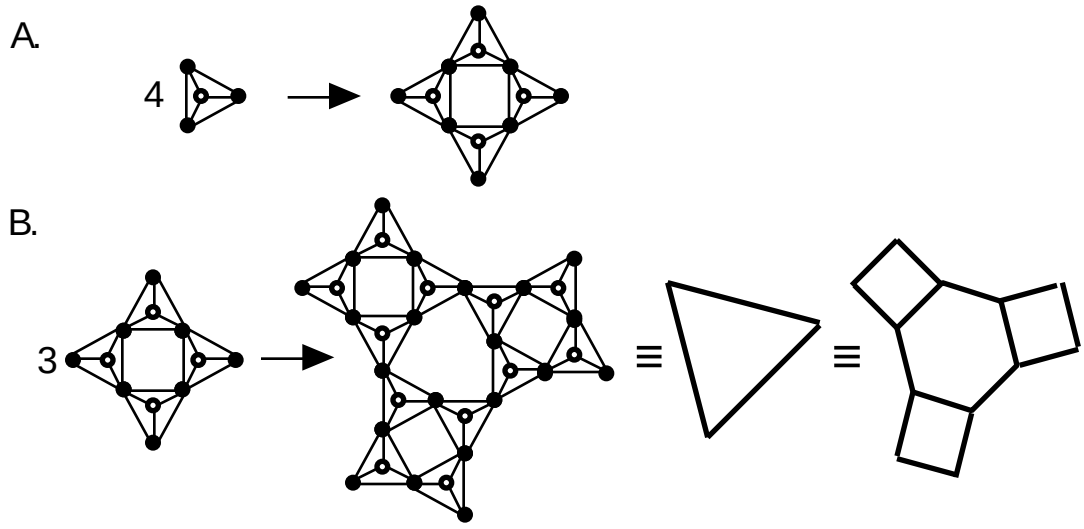

Figure 5.35A–B. Construction of zeolites by linking SiO_4^{4-} tetrahedra. A: Linking of four tetrahedra produces a square of tetrahedra. B: Linking of three squares generated in A produces a structure in which an interior hexagon of silicon atoms is formed. Like the triangle shown, this structure is analogous to one face of an octahedron. This shape may also be represented by a hexagon with squares fused to alternate edges; this representation shows only the positions of the silicon atoms, which are located at the vertices of the hexagons and squares. *(Continued on next page.)*

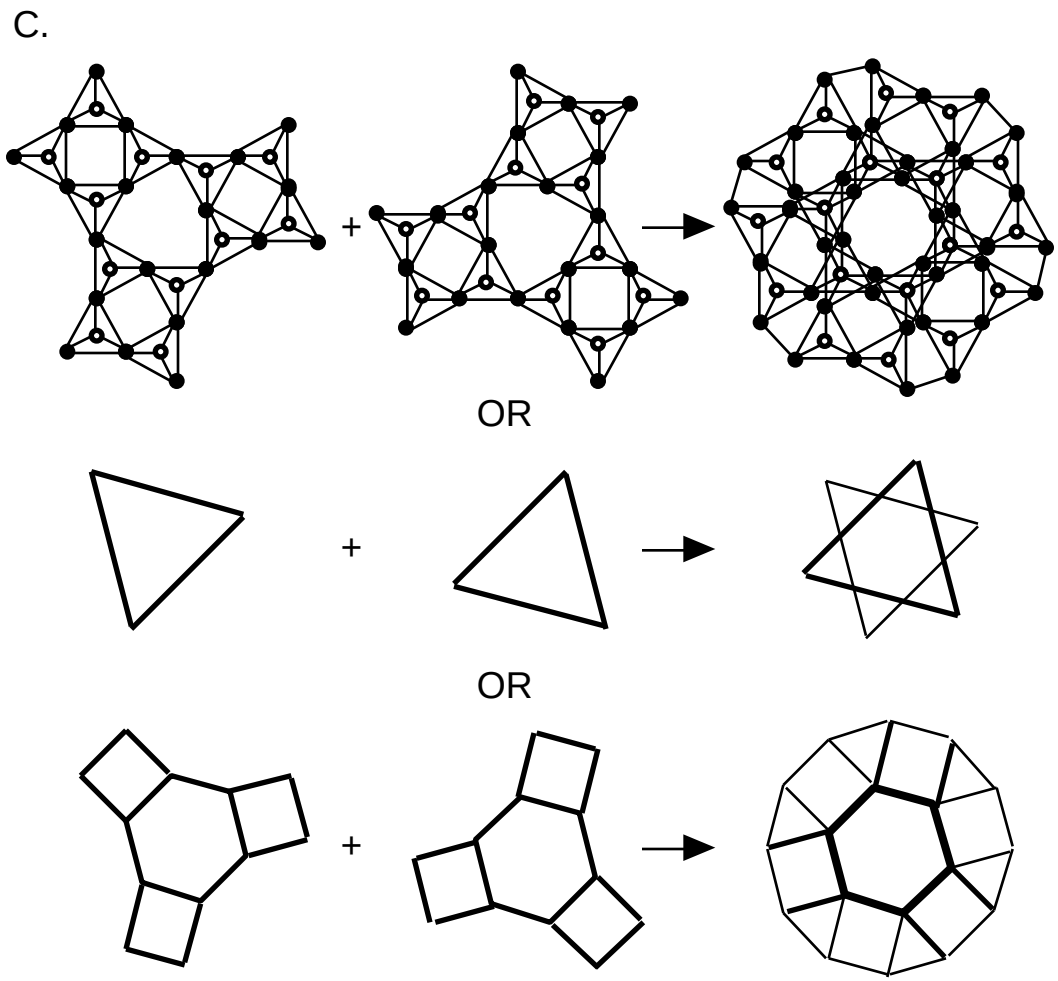

Figure 5.35C. Superposition of the shapes described in B with one oriented at 60° to it and above it, followed by fusion of the two frameworks at the appropriate points, generates shapes that have octahedral symmetry. In the silicate, the shape that is generated has a square of silicon atoms at each vertex of an octahedron and a hexagon on each face. This shape is a sodalite unit of a zeolite structure and is analogous to the superposition of one triangle with another oriented at 60° to it and above it, which generates an octahedron. Generation of the resulting silicate framework may also be viewed by showing only the positions of the silicon atoms.

The linkage of tetrahedra at all four corners generates SiO_2, silica, which exists in at least three crystalline forms—quartz, cristobalite♦ and tridymite♦. The sketches in Figures 5.37 and 5.38 show how the SiO_4^{4-} tetrahedra are linked through their corners to produce the structure of quartz and cristobalite, respectively.

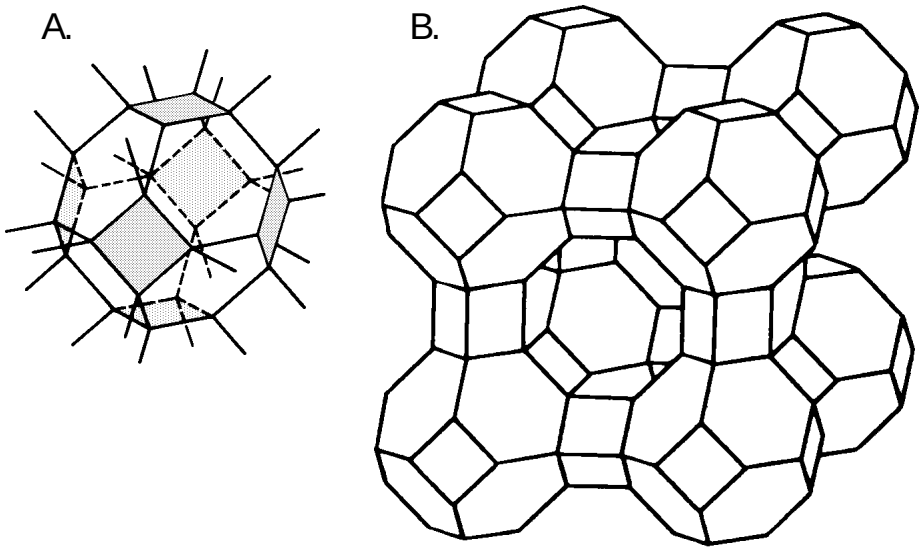

Figure 5.36. A: A sodalite unit. The lines coming out from the shape represent oxygen atoms that are available for additional linking. B: Linking of eight sodalite units generates a zeolite. This structure, similar to a simple cubic lattice, extends in three dimensions. A series of open pores runs through the structure.

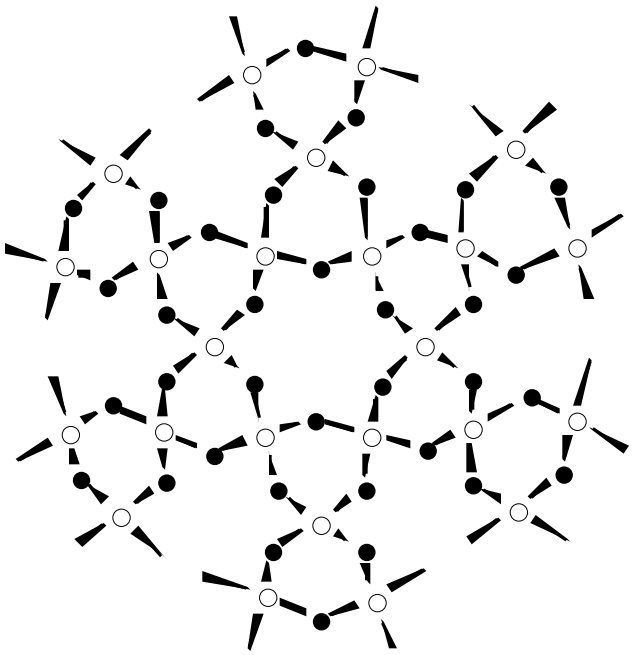

Figure 5.37. The SiO_2 (β-quartz) structure, viewed down the helical axis. The open circles represent silicon atoms and the closed circles represent oxygen atoms.

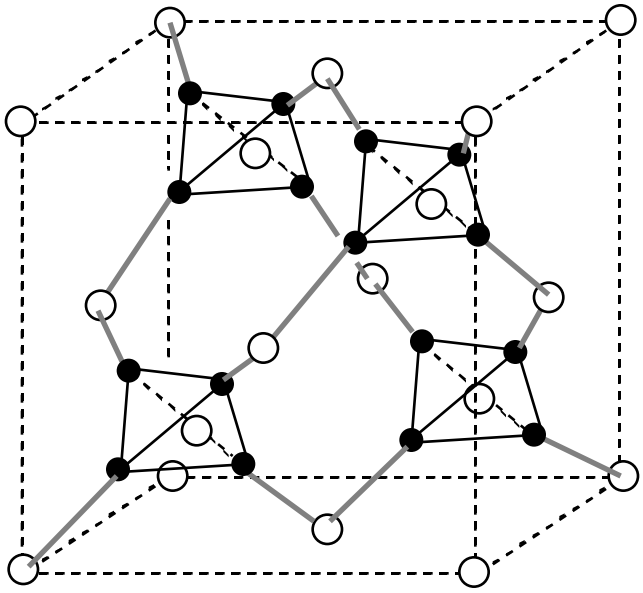

Figure 5.38. The SiO_2 (cristobalite) structure. The atoms in the corners and faces of the cube are silicon (open circles). Some of the surrounding tetrahedra of oxygen atoms (filled circles) have been omitted for clarity.

Appendix 5.1. The ICE Solid-State Model Kit

The SSMK makes use of a base with holes, a template to cover a subset of those holes, and radius-ratio size spheres that slide down rods inserted in holes in the base.

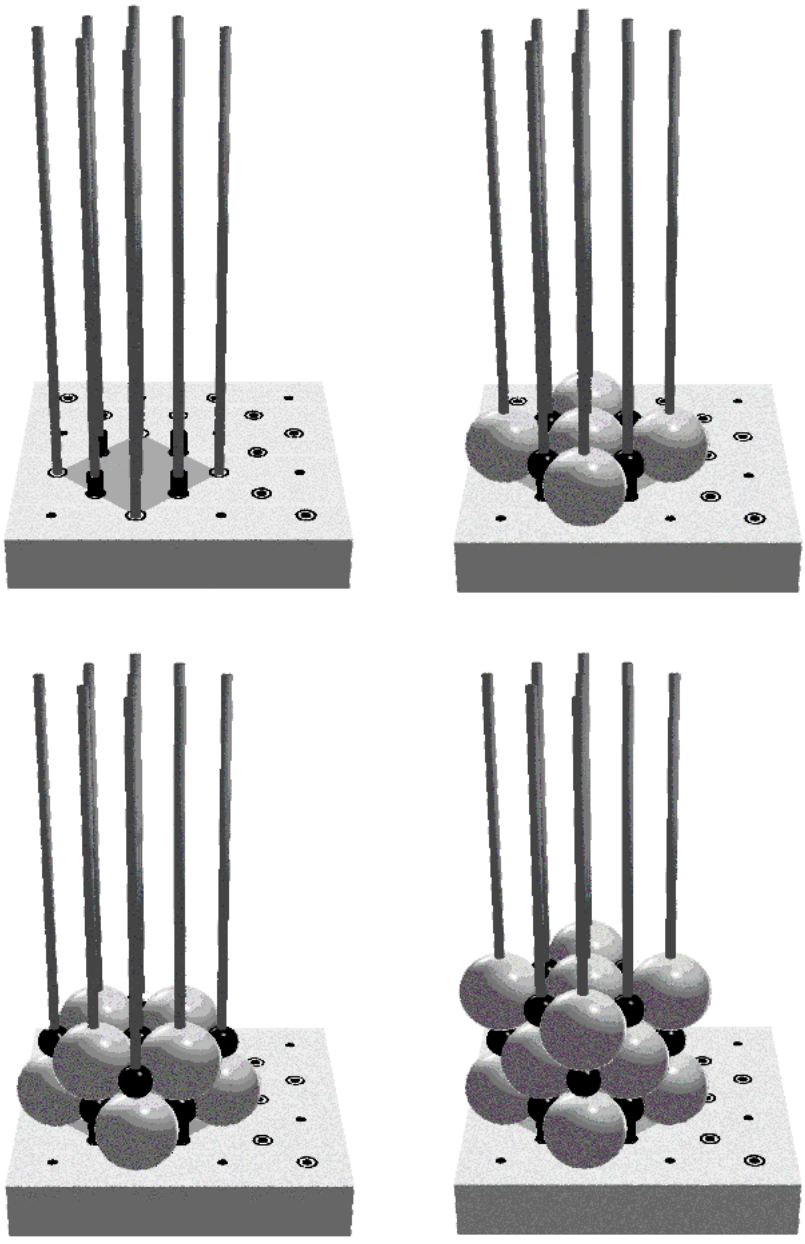

Appendix 5.2. Solid-State Structures and MacMolecule

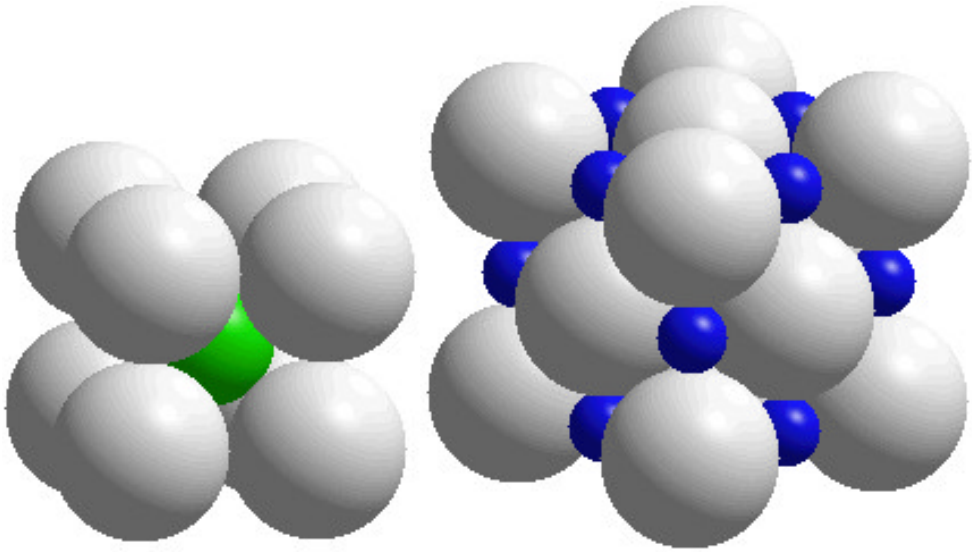

CsCl NaCl

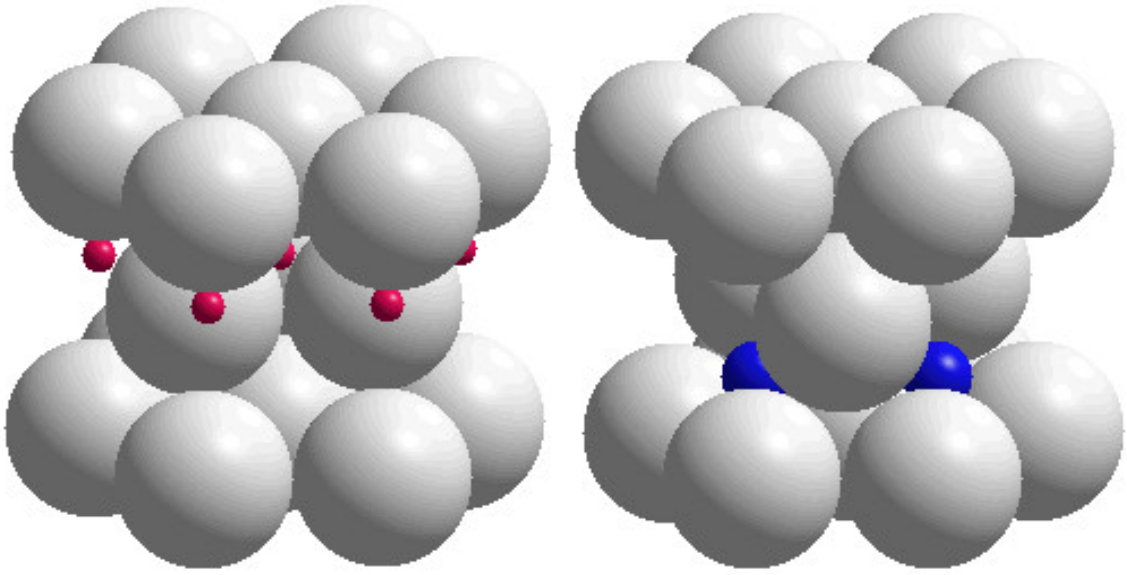

ZnS (wurtzite) CdI_2

Images created with MacMolecule.

A collection of data files for the MacMolecule program has been prepared by Ludwig Mayer, Department of Chemistry, San Jose State University, San Jose, CA 95192–0101. MacMolecule (by Eugene Myers and Carlos Blanco, Department of Computer Science, and Richard B. Hallick and

Jerome Jahnke, Departments of Biochemistry and Molecular and Cellular Biology, University of Arizona, Tucson, AZ 85721) provides the capability to display, rotate, and examine molecular images in real time. Sample black-and-white images are shown here, but the program runs in color on Macintosh computers. MacMolecule can be obtained by anonymous FTP at joplin.biosci.arizona.edu. User-contributed image files will also be made available at this address in the /pub/MacMolecule directory, and bundled with future releases.

Appendix 5.3. Bubble Raft Construction

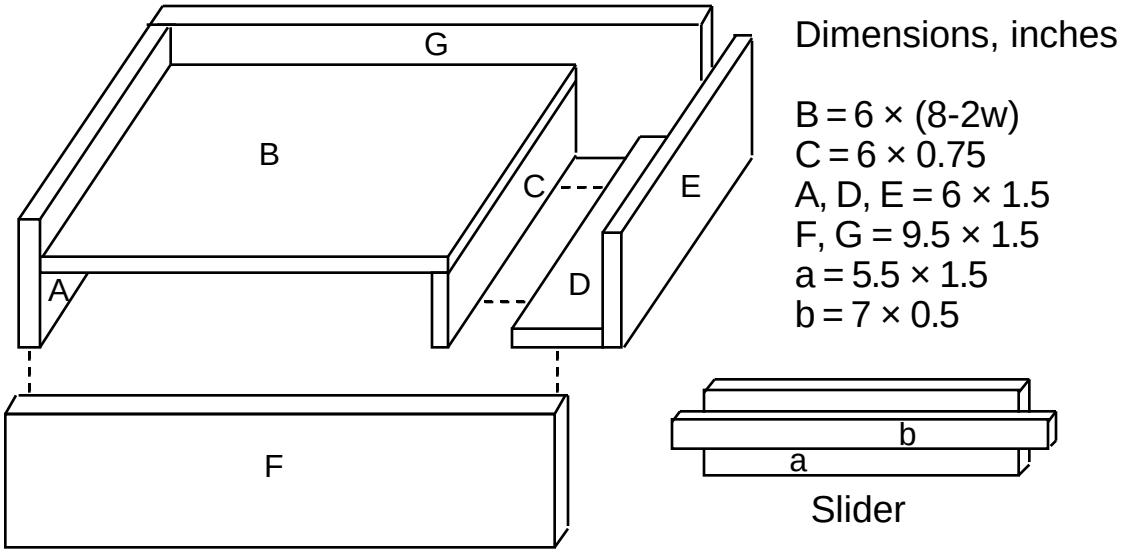

In piece B, *w* is the width of Plexiglas used; 1/8-inch Plexiglas is sufficient for the construction of the bubble raft.

Appendix 5.4. Tetrahedral and Octahedral Models

Cut out model. Use a pen and ruler to score along lines. Fold away from lines to assemble.

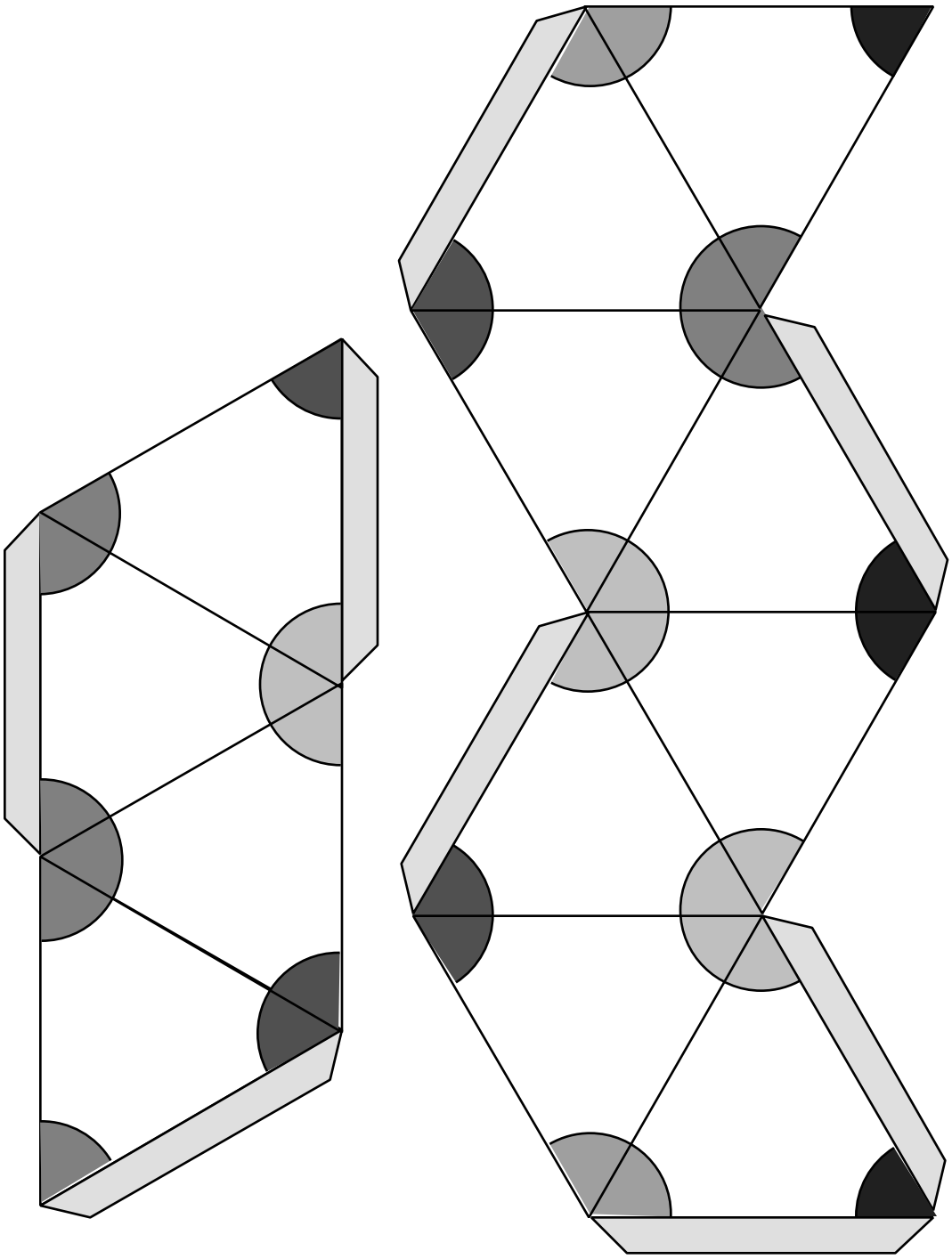

Appendix 5.5. Crystal Habits

The habit or shape of a crystal is determined by the rate at which different faces grow; the fastest growing faces are eliminated. When cubic faces (shaded) grow the fastest, they can produce an octahedral or a tetrahedral habit. (Adapted from reference 7.)

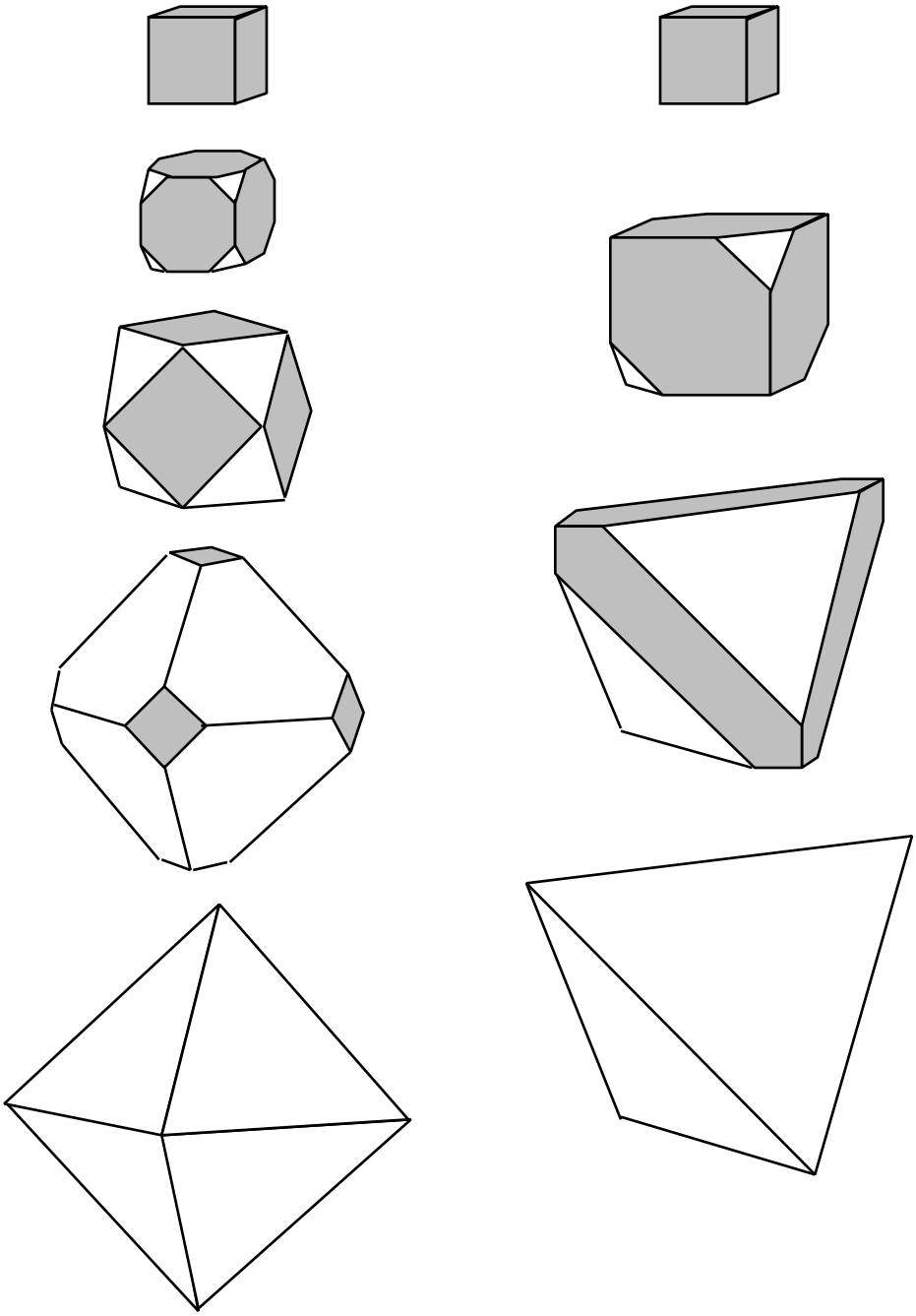

Appendix 5.6. Elements and Compounds That Exhibit the Common Structural Types

Elements

Diamond Structure♦

C	3.56683
Si	5.43072
Ge	5.65754
α-Sn	6.4912

Body-Centered Cubic♦

Ba	5.025	Li	3.5093	Ta	3.3058
Cr	2.8839	Mo	3.1473	V	3.0240
Cs	6.045 (5 K)	Na	4.2906	W	3.16469
α-Fe	2.8665	Nb	3.3004		
K	5.225 (5 K)	Rb	5.585 (5 K)		

Cubic Close-Packed♦

Ac	5.311	In	3.244	Pd	3.8898
Ag	4.0862	Ir	3.8394	Pt	3.9231
Al	4.04958	Kr	5.721 (58 K)	Rh	3.8031
Ar	5.256 (4.2 K)	Ne	4.429 (4.2 K)	Xe	6.197 (58 K)
Au	4.07825	Ni	3.52387		
Cu	3.61496	Pb	4.9505		

Hexagonal Close-Packed♦

Be, β-Ca, Cd, α-Co, Hf, Mg, Os, Re, Ru, Sc, β-Sr, Tc, Ti, Tl, Y, Zn, α-Zr

Compounds

CsCl Structure♦

AgCd	3.33	CsBr	4.286	MgTl	3.628
AgMg	3.28	CsCl	4.123	NiAl	2.881
AgZn	3.156	CsI	4.5667	NiTi	3.01 (austenite)
AuMg	3.259	CuPd	2.988	SrTl	4.024
AuZn	3.19	CuZn	2.945	TlBi	3.98
BeCo	2.606	LiAg	3.168	TlBr	3.97
BeCu	2.698	LiHg	3.287	TlCl	3.8340
BePd	2.813	LiTl	3.424	TlI	4.198
CaTl	3.847	MgHg	3.44	TlSb	3.84
CoAl	2.862	MgSr	3.900		

NaCl Structure♦

AgBr	5.7745	MgO	4.2112	SnAs	5.681
AgCl	5.547	MgS	5.2023	SnSb	6.130
AgF	4.92	MgSe	5.451	SnSe	6.020
BaO	5.523	MnO	4.4448	SnTe	6.313
BaS	6.3875	MnS	5.2236	SrO	5.1602
BaSe	6.600	MnSe	5.448	SrS	6.0198
BaTe	6.986	NaBr	5.97324	SrSe	6.23
CaO	4.8105	NaCl	5.62779	SrTe	6.47
CaS	5.6903	NaF	4.620	TaC	4.4540
CaSe	5.91	NaH	4.880	TaO	4.422
CaTe	6.345	NaI	6.4728	TiC	4.3186
CdO	4.6953	NbC	4.4691	TiN	4.235
CoO	4.2667	NbO	4.2097	TiO	4.1766
CrN	4.410	NiO	4.1684	VC	4.182
CsF	6.008	PbS	5.9362	VN	4.128
CsH	6.376	PbSe	6.1243	YAs	5.786
KBr	6.6000	PbTe	6.454	YN	4.877
KCl	6.29294	PdH	4.02	YTe	6.095
KF	5.347	RbBr	6.854	ZrB	4.65
KH	5.700	RbCl	6.5810	ZrC	4.6828
KI	7.06555	RbF	5.64	ZrN	4.567
LiBr	5.5013	RbH	6.037	ZrO	4.62
LiCl	5.12954	RbI	7.342	ZrP	5.27
LiF	4.0173	ScAs	5.487	ZrS	5.250
LiH	4.085	ScN	4.44		
LiI	6.000	ScSb	5.859		

Fluorite and Anti-Fluorite Structure♦

$AuAl_2$	6.00	K_2S	7.391	$PtGa_2$	5.911
$AuGa_2$	6.063	K_2Se	7.676	$PtIn_2$	6.353
$AuIn_2$	6.502	K_2Te	8.152	$PtSn_2$	6.425
$AuSb_2$	6.656	Li_2O	4.619	RaF_2	6.368
$BaCl_2$	7.34	Li_2S	5.708	Rb_2O	6.74
BaF_2	6.2001	Li_2Se	6.005	Rb_2S	7.65
Be_2B	4.670	Li_2Te	6.504	Rb_2P	5.505
Be_2C	4.33	Na_2O	5.55	ScH_2	4.78315
CaF_2	5.46295	Na_2S	6.526	$SiMg_2$	6.39
CdF_2	5.3880	Na_2Se	6.809	SmH_2	5.376
$CoSi_2$	5.356	Na_2Te	7.314	$SnMg_2$	6.765
$GeMg_2$	6.378	NbH_2	4.563	$SrCl_2$	6.9767
HfO_2	5.115	$NiSi_2$	5.395	SrF_2	5.7996
HgF_2	5.54	β-PbF_2	5.92732	YH_2	5.199
$IrSn_2$	6.338	$PbMg_2$	6.836	ZrO_2	5.07
Ir_2P	5.535	α-PoO_2	5.687		
K_2O	6.436	$PtAl_2$	5.910		

Zinc Blende Structure♦

AgI	6.473	CdS	5.832	HgTe	6.4623
AlAs	5.6622	CdSe	6.05	InAs	6.05838
AlP	5.451	CdTe	6.477	InP	5.86875
AlSb	6.1347	CuBr	5.6905	InSb	6.47877
BAs	4.777	CuCl	5.4057	MnS	5.011
BN	3.615	CuF	4.255	MnSe	5.82
BP	4.538	CuI	6.0427	SiC	4.348
BePo	5.838	GaAs	5.65315	ZnPo	6.309
BeS	4.865	GaP	5.4505	ZnS	5.4093
BeSe	5.139	GaSb	6.0954	ZnSe	5.6676
BeTe	5.626	HgS	5.8517	ZnTe	6.101
CdPo	6.665	HgSe	6.084		

ReO_3 Structure♦

MoF_3	3.8985
NbF_3	3.903
ReO_3	3.734
TaF_3	3.9012

Perovskite Structure♦

$AgZnF_3$	3.98	$KCoF_3$	4.069	$SmFeO_3$	3.845
$BaFeO_3$	4.012	$KFeF_3$	4.122	$SmVO_3$	3.89
$BaMoO_3$	4.0404	$KMgF_3$	3.973	$SrFeO_3$	3.869
$BaPbO_3$	4.273	$KMnF_3$	4.190	$SrHfO_3$	4.069
$BaSnO_3$	4.1168	$KTaO_3$	3.9885	$SrMoO_3$	3.9751
$BaTiO_3$	4.0118 (201 C)	$LiBaF_3$	3.996	$SrSnO_3$	4.0334
$BaZrO_3$	4.1929	$LiBaH_3$	4.023	$SrTiO_3$	3.9051
$CaSnO_3$	3.92	$NaAlO_3$	3.73	$SrZrO_3$	4.101
$CaTiO_3$	3.84	$NaWO_3$	3.8622	$TaSnO_3$	3.880
$CaVO_3$	3.76	$RbCaF_3$	4.452	$TlCoF_3$	4.138
$CaZrO_3$	4.020	$RbCoF_3$	4.062	$TlIO_3$	4.510
$CsCaF_3$	4.522	$RbMnF_3$	4.250	$YCrO_3$	3.768
$CsCdF_3$	5.20	$SmAlO_3$	3.734	$YFeO_3$	3.785
$CsPbBr_3$	5.874	$SmCoO_3$	3.75		
$KCdF_3$	4.293	$SmCrO_3$	3.812		

Wurtzite Structure♦

AgI, AlN, BeO, CdS, CdSe, CuBr, CuCl, CuH, CuI, GaN, InN, MgTe, MnS, MnSe, MnTe, NbN, SiC, TaN, ZnO, ZnS, ZnSe, ZnTe

NiAs Structure♦

AuSn, CoS, CoSb, CoSe, CoTe, CrSb, CrSe, CrTe, CuSn, FeS, FeSb, FeSe, FeTe, IrSb, IrTe, MnAs, MnBi, MnSb, MnTe, NiAs, NiSb, NiSe, NiTe, PdSb, PdTe, PtB, PtSb, PtSn, RhBi, RhTe, ScTe, TiS, TiSe, TiTe, VP, VS, VSe, ZrTe

CdI_2 Structure♦

Ag_2F, CaI_2, CdI_2, $CoBr_2$, CoI_2, $CoTe_2$, $FeBr_2$, FeI_2, GeI_2, HfS_2, $HfSe_2$, $IrTe_2$, $MgBr_2$, MgI_2, $MnBr_2$, MnI_2, $NiTe_2$, PdI_2, $PdTe_2$, PtS_2, $PtSe_2$, $PtTe_2$, $SiTe_2$, SnS_2, $SnSe_2$, α-TaS_2, $TiBr_2$, $TiCl_2$, TiI_2, $TiSe_2$, TiI_2, $TiSe_2$, $TiTe_2$, VBr_2, VCl_2, VI_2, W_2C, ZrS_2, $ZrSe_2$, $ZrTe_2$

NOTE: For cubic unit cells, the edge length is given in angstroms.
SOURCE: Data were obtained from references 11–14.

Appendix 5.7. Synthesis and Reactivity of $AuAl_2$

Synthesis

Aluminum spheres cut to expose fresh surfaces (0.100 g, 0.00371 mol) and powdered gold (0.365 g, 0.00185 mol) are placed in a ~6-mm i.d. quartz tube that has been shaped into a V. One end of the tube is connected to Tygon tubing, through which nitrogen is passed to purge oxygen from the system. While using a very slow nitrogen purge (six bubbles per minute), the metals are heated with a Meker burner in a fume hood. **Caution! Once the aluminum melts, the highly exothermic reaction will proceed quickly** to produce a purple, metallic solid.

Reactivity

$AuAl_2$ will react with 3M HCl to dissolve the aluminum and generate hydrogen gas, leaving behind gold powder. It will also react with 50% NaOH to yield $Al(OH)_4^-{}_{(aq)}$ and gold powder.

References

1. Bragg, L.; Nye, J. F. *Proc. Roy. Soc. London* **1947**, *190*, 474–481.
2. The soap solution is based on recipes found in the following sources: *Scienceworks*; Ontario Science Centre; Addison-Wesley: Reading, MA, 1984; p 84; Katz, D. A. *Chemistry in the Toy Store*, 5th ed.; Doherty, P.; Rathjen, D., Eds.; Community College of Philadelphia: Philadelphia, PA, 1990; *Exploratorium Science Snackbook*; Exploratorium Teacher Institute: San Francisco, CA, 1991; p 16.
3. Nathan, L. C. *J. Chem. Educ.* **1985**, *62*, 215.
4. Smart, L.; Moore, E. *Solid State Chemistry*; Chapman and Hall: London, 1992; p 39.
5. Burdett, J. K.; Price, S. L.; Price, G. D. *Solid State Comm.* **1981**, *40*, p 923.
6. Massey, A. G. *Main Group Chemistry*; Ellis Harwood Ltd. Chichester, England, 1990; p 228.
7. Holden, A.; Singer, P. *Crystals and Crystal Growing*; Anchor: Garden City, NY, 1960.
8. Sharma, B. D. *J. Chem. Educ.* **1987**, *64*, 404–407.
9. Jolly, W. L. *Modern Inorganic Chemistry*; McGraw-Hill: New York, 1984; p 275.
10. Gehman, W. *J. Chem. Educ.* **1963**, *40*, 54–60.
11. Wells, A. F. *Structural Inorganic Chemistry*, 5th ed.; Oxford University Press: Oxford, England, 1984.
12. Wyckoff, R. W. G. *Crystal Structures*, 2nd ed.; Interscience Publishers: New York, 1963, Vol. 1.
13. *CRC Handbook of Chemistry and Physics*, 68th ed.; Weast, R. C., Ed.; CRC Press: Boca Raton, FL, 1987.
14. Galasso, F. S. *Structure and Properties of Inorganic Solids*; Pergamon Press: Oxford, 1970.

Additional Reading

Bubble Raft

· Bragg, L.; Nye, J. F. *Proc. Roy. Soc. London* **1947**, *190*, 474; reprinted in Feynman, R. P.; Leighton, R. B.; Sands, M. *The Feynman Lectures on Physics*; Addison Wesley: Reading, MA, 1964; Vol. II, Chapter 30, p 10.

Structure

· Galasso, F. S. *Structure and Properties of Inorganic Solids*; Pergamon Press: Oxford, England, 1970.
· Smart, L.; Moore, E. *Solid State Chemistry: An Introduction*; Chapman and Hall: London, 1992.

· Wells, A. F. *Structural Inorganic Chemistry*, 5th ed.; Oxford University Press: Oxford, England, 1984.
· West, A. R. *Solid State Chemistry and Its Applications*; John Wiley and Sons: New York, 1984.

Acknowledgments

We thank Jill Banfield, University of Wisconsin—Madison, Department of Geology and Geophysics, for helpful comments on this chapter.

Exercises

1. Determine the packing efficiency of a simple cubic cell that contains one metal atom with a diameter of 1.00 Å as follows:
   a. Calculate the volume of the atoms that are contained in the cell. For a sphere, $V = (4/3)\pi r^3$.
   b. Determine the length of the cell edge in terms of the diameter of the atom contained in the unit cell. Hint: consider where the atoms touch each other.
   c. Determine the volume of the cubic unit cell.
   d. Determine the packing efficiency for the simple cubic structure.
2. Determine the packing efficiency of a body-centered cubic cell that contains metal atoms with a diameter of 1.00 Å as follows:
   a. Calculate the volume of the atoms that are contained in the cell. For a sphere, $V = (4/3)\pi r^3$.
   b. Determine the length of the cell edge in terms of the diameter of the atom contained in the unit cell. Hint: notice that the atoms touch each other along the body diagonal of the unit cell.
   c. Determine the volume of the cubic unit cell.
   d. Determine the packing efficiency for the structure.
3. Determine the packing efficiency of a face-centered cubic cell that contains metal atoms with a diameter of 1.00 Å using the steps described in Exercise 2. Hint: notice that the atoms touch each other along the face diagonal of the unit cell.
4. Which of the following is <u>not</u> characterized by a tetrahedral structure?
   a. CH_4
   b. Zn^{2+} ions in a cubic close-packed structure of S^{2-} ions
   c. a C atom in the diamond crystal structure
   d. Na^+ ions in a cubic close-packed structure of Cl^- ions
5. How does the CsCl structure change as one goes from the unit cell shown in Figure 5.12A to that in Figure 5.12B?
6. Estimate the radius of a hydride ion in LiH using the data in Appendix 5.6. Assume that the hydride ions touch in the structure.
7. Determine the density of any of the compounds or elements in Appendix 5.6 from the formula, structure type, and unit-cell dimension.
8. What is the formula of a compound that crystallizes with zinc atoms occupying one-half of the tetrahedral holes in a cubic close-packed array of sulfur atoms?

(Zn and S can be replaced by any of the pairs listed for the Zinc Blende structure in Appendix 5.6.)

9. What is the formula of a compound that crystallizes with lithium ions occupying all of the tetrahedral holes in a cubic close-packed array of sulfide ions? (Li and S can be replaced by any of the pairs listed for the antifluorite structure in Appendix 5.6.)
10. What is the formula of a compound that crystallizes with silver ions occupying all of the octahedral holes in a cubic close-packed array of chloride ions? (Ag and Cl can be replaced by the ions of any of the pairs listed for the NaCl structure in Appendix 5.6.)
11. What is the formula of a compound that crystallizes with thallium ions occupying all of the cubic holes in a simple cubic array of iodide ions? (Tl and I can be replaced by the ions of any of the pairs listed for the CsCl structure in Appendix 5.6.)
12. What is the formula of a compound that crystallizes with barium ions occupying one-half of the cubic holes in a simple cubic array of fluoride ions? (Ba and F can be replaced by the ions of any of the pairs listed for the fluorite structure in Appendix 5.6.)
13. Consider cubic crystals of CsCl, NaCl, ZnS, CaF_2, and $CaTiO_3$.
    a. Sketch the STM trace of the face of the crystal, assuming that the STM tip travels three unit cells in each of the two directions.
    b. Assume that crystals of each compound in part a are cleaved so the atoms at $z = 0.5$ are exposed. Sketch the STM trace of each, assuming that the STM tip travels three unit cells in each of the two directions.
    c. Assume that crystals of CaF_2 and ZnS are cleaved so the atoms at $z = 0.25$ are exposed. Sketch the STM trace of each, assuming that the STM tip travels three unit cells in each of the two directions.
14. Calculate the radius of an atom of any of the metals whose unit-cell dimensions are given in Appendix 5.6.
15. The atomic radii of carbon, silicon, and germanium are approximately 0.77 Å, 1.17 Å, and 1.22 Å, respectively. *Calculate* the covalent radius (r) of carbon, silicon, or germanium by referring to the X-ray diffraction data in Appendix 5.6 and the structure shown in Figure 5.24 (Hint: Each of the four atoms contained within the body of the unit cell touches three face-centered atoms and one corner atom for tetrahedral coordination. Try subdividing the unit cell into eight smaller cubes; the body diagonal of each small cube will have a length of 4r.)
16. Determine the ionic radius of the metal ion in any of the oxides in Appendix 5.6 with the NaCl structure.
17. Assume that the radius of the bromide ion is unknown and determine it from a plot of unit cell volume versus anion volume for KF, KCl, KBr, and KI; or NaF, NaCl, NaBr, and NaI. The radii of the F, Cl, and I anions are 1.19, 1.67, and 2.06 Å, respectively. (This exercise can be repeated for any series of isostructural compounds with one missing ionic radius. For example, the radius of Co may be determined from plots involving oxides with the NaCl structure found in Appendix 5.6 and the ionic radius of 1.26 Å for O^{2-}.)
18. Which of these metals contain undistorted cubic holes? octahedral holes? tetrahedral holes? Al, Ba, Co, Fe, Mo, Pb, Po (*see* Figure 3.11).
19. An anisotropic structure is one that has bonding or structural units along one of its unit cell directions that differ from the bonding or structural units along one or both of the other unit cell directions. From the examples in this chapter

give an example of an ionic compound that is anisotropic and one that is not; of a covalent solid that is anisotropic and one that is not.

20. Aluminum is composed of larger and lighter atoms than silicon. Why is the density of aluminum larger than that of silicon?
21. The geometry of a close-packed plane of atoms in a hcp structure is identical to that of a close-packed plane of atoms in a ccp structure. Why do the structures differ?
22. Graphite and diamond contain carbon atoms with coordination numbers of 3 and 4, respectively. However, the radius ratio rule predicts that the coordination number should be 8 or 12 for both substances. Why does carbon in diamond or graphite form differ from the prediction?
23. Several factors can cause a structure to differ from that predicted from the radius ratio rule. Using the radius ratio rule, what coordination number is predicted for silicon in elemental silicon? Why does silicon not exhibit this coordination number?
24. In the figure caption for Figure 5.15 (the $CdCl_2$ structure) the statement is made that the picture shown does not represent a complete unit cell. Show that the picture is not consistent with the $CdCl_2$ stoichiometry.
25. Use the packing diagrams shown in the figures for this chapter to determine the contents of the unit cell and verify the formulas for
    a. NiAs
    b. NaCl
    c. CdI_2
    d. Li_2O
    e. CaF_2
26. What sort of cleavage properties would you expect for a single crystal of CdI_2?
27. Use Figure 5.23 to show that there are two tetrahedral holes and one octahedral hole per atom in a hcp unit cell.
28. Use Figures 5.13 and 5.19 to show that there are two tetrahedral holes and one octahedral hole per close-packed sphere in a fcc crystal.
29. K_xC_{60} has potassium atoms that completely fill the octahedral and tetrahedral holes in a fcc arrangement of C_{60} anions. What is the value of x in K_xC_{60}?
30. Generate a z-layer sequence for ReO_3 (Figure 5.27A).
31. Confirm the formula of the superconductor shown in Figure 5.29C.
32. Confirm the formula of the silicate repeat units in Figures 5.31, 5.32, and 5.33, using the atom sharing formalisms developed for unit cells.
33. The amphibole structure has the silicate repeat unit formula $(Si_4O_{11}^{6-})_n$. If there is isomorphous substitution in which aluminum atoms replace (a) 25%, or (b) 50% of the silicon atoms, what will the charge be on the repeat unit?
34. The octahedral ferrocyanide ion, $Fe(CN)_6^{4-}$, forms an insoluble salt with Fe^{3+}. This salt is intensely colored and called Prussian blue. In the crystal structure there are linear Fe^{2+}–C–N–Fe^{3+} arrays of atoms.
    a. Crystals of Prussian blue have the NaCl-like structure, with Fe^{3+} in the Na^+ site and $Fe(CN)_6^{4-}$ in the Cl^- site. If Prussian blue had the perfect NaCl structure, how many Fe^{3+} ions would surround the $Fe(CN)_6^{4-}$ ions?
    b. What is the formula for Prussian blue? In other words, what are x and y in $[Fe^{3+}]_x[Fe(CN)_6^{4-}]_y$?
    c. Given your answer in b, why is it impossible for Prussian blue to have a perfect NaCl structure?
35. The text discussed tetrahedral and octahedral holes in close-packed structures. There are also trigonal (three-coordinate) holes with a single layer of a close-packed structure. Draw one close-packed layer and indicate the location of a trigonal planar hole.

36. In α-aluminum oxide, there is a hcp array of oxide ions with two-thirds of the octahedral holes filled with aluminum ions. What is the formula of α–aluminum oxide?
37. A mercury iodide salt can be described as a ccp array of iodide ions with one-fourth of the tetrahedral holes occupied by mercury ions. What is the formula for this salt?
38. A tin iodide salt consists of a ccp array of iodide ions with Sn ions in one-eighth of the tetrahedral holes. What is its formula?
39. Aluminum selenide can be described as selenide ions in a hcp array with aluminum ions in one-third of the tetrahedral holes. What is its formula?
40. An early attempt to develop a set of ionic radii was made by Lande in 1920. He assumed that Li^+ would be the smallest ion found in crystals and that in compounds with the largest halide ions, the lithium ion would be too small to keep the halide ions from touching. Thus, knowledge of the crystal structure and unit-cell dimensions provided a method for an estimation of the lithium and iodide ionic radii.
    a. Draw a picture of the $z = 0$ layer sequence for LiI. (*See* Appendix 5.6 for the crystal structure adopted by LiI and subsequent compounds required for this problem.)
    b. Use the picture you have generated to calculate the ionic radius of iodide, using the unit cell dimensions given in Appendix 5.6 and assuming that the iodide ions are just touching.
    c. Use the calculated ionic radius of iodide and the picture you drew in part a to estimate the radius of Li^+.
    d. Using these two ionic radii, calculate the ionic radii for the alkali metals and the halide ions.
41. The structure of MoS_2 is illustrated in Figure 5.26. In which directions will planes of atoms in MoS_2 slip most easily?
42. The structure of graphite is illustrated in Figure 5.25. In which direction will planes of atoms in graphite slip most easily?
43. Discuss the relationship between the atom positions in the following structures (some of these are shown in the Chapter 3 exercises):
    a. NaCl and CaC_2
    b. MgAgAs and ZnS (Zinc Blende)
    c. CdI_2 and NiAs
44. How many nearest neighbors does each atom have in a bcc structure? in a fcc structure?

45. Graphite can be viewed as a polymerized version of benzene. There is a polymorph of boron nitride that can be viewed as a polymerized version of borazine. Hexagonal boron nitride and graphite are both layered solids that are good lubricants, but boron nitride is white and has a higher oxidation temperature (850 °C).

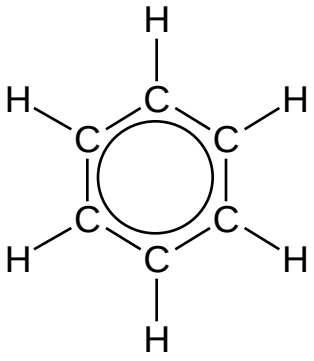

Benzene

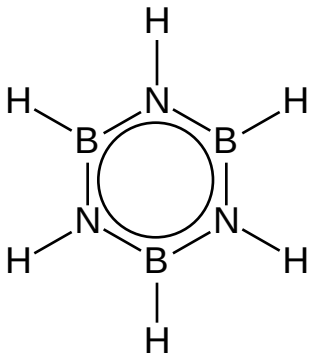

Borazine

a. Draw a layer of hexagonal boron nitride by analogy to graphite.
b. The structure of graphite and hexagonal boron nitride differ since the boron nitride layers stack directly over each other (with alternating B N B N... stacking) and are eclipsed rather than staggered as in graphite. Make a sketch analogous to Figure 5.25B that shows the structure of hexagonal boron nitride.

46. Which of the layer sequences below corresponds to face-centered cubic, hexagonal close packing, and cubic close packing unit cells? How many total atoms are there within each of these unit cells?